Ph.D. Dissertation of Engineering

Flood mitigation effect of green-gray infrastructures in urban area

도시 지역에서의 그린-그레이 인프라 홍수 완화 효과

August 2022

Graduate School of Seoul National University
Interdisciplinary Program in Landscape Architecture
Integrated Major in Smart City Global Convergence Program

Chaeyoung Bae

Flood mitigation effect of green-gray infrastructures in urban area

Advisor: Dong Kun Lee

A dissertation submitted in partial fulfillment of the requirements for the Degree of Doctor of Philosophy in Interdisciplinary Program in Landscape Architecture and Integrated Major in Smart City Global Convergence Program in Seoul National University

August 2022

Chaeyoung Bae

Approved by Thesis Committee

Chair ____________(Seal)

Vice Chair____________(Seal)

Examiner ____________(Seal)

Examiner ____________(Seal)

Examiner ____________(Seal)

Abstract

Flood mitigation effect of green-gray infrastructures in urban area

Chaeyoung Bae
Interdisciplinary Program in Landscape Architecture and
Integrated Major in Smart City Global Convergence Program in
Seoul National University
Graduate School of Seoul National University
Supervised by Professor Dong Kun Lee

The existing methods for mitigating urban flooding have focused on the volume expansion of sewerage systems, however, these measures alone are expensive and primarily aimed at water treatment, making them an unsustainable solution to unpredictable rainfall. Thus, strategies have been proposed and applied over the past decade to control runoff and delay peak flow by restoring natural hydrologic circulation and maximizing infiltration and retention capacities at the source. In this study, using the green infrastructure (GI) concept, a model simulation was conducted to quantify the effects of green-gray infrastructure on flood mitigation by changes in different techniques, rainfall patterns, and implementation location.

Therefore, the main research question for each chapter in this paper is: 1) Is the green infrastructure effective in flood reduction? 2) How does the effect differ according to various rainfall patterns, and how does the effect differ when integrated with the gray infrastructure, 3) How does the effect differ depending on the where the green-gray infrastructure practices are implemented? This study used a deterministic hydrologic model to perform a before-and-after analysis of hypothetical scenarios such as various rainfall, technology, and location.

The results of this study are significant as they improve model accuracy through parameter optimization and model correction considering both past and current time points, and quantify the potential effect of GI technology based on flood events of various characteristics. In addition, it emphasizes the importance of detailed comparisons of various options in the decision-making process related to green-gray infrastructure planning.

Keyword: Green infrastructure, urban flood management, urban drainage system, deterministic modeling, spatial and temporal effect

Student Number: 2019-35254

Table of Content

Abstract i

List of Figures v

List of Tables vi

I. Introduction 1

II. Effects of low-impact development practices for flood events at the catchment scale in a highly developed urban area 6

2.1 Introduction 6

2.2 Methods 9

2.2.1 Study site 9

2.2.2 Urban rainfall-runoff modeling 12

2.2.3 Low-impact development 16

2.3 Results and discussion 19

2.3.1 Model updating 19

2.3.2 Effects of LID practices on flood events 22

2.4 Conclusions 27

III. Quantifying the effect of green-gray infrastructure at the catchment scale under various rainfall patterns 29

3.1. Introduction 29

3.2. Materials and Methods 32

3.2.1 Case study 32

3.2.2 Applied meteorological data 33

3.2.3 Hydrological assessment 35

3.2.4 Green-gray infrastructure 37
3.2.5 Time-dependent resilience assessment 40
3.3. Results and Discussion 42
3.3.1 Calibration of the model 42
3.3.2 Effectiveness of green infrastructure implementation 44
3.3.3 Effectiveness of green-gray infrastructure implementation 47
3.3.4 Flood resilience 49
3.4. Conclusions 51
IV. Optimized placement of green-gray infrastructure for effective flood mitigation 53
4.1. Introduction 53
4.2. Methods 56
4.2.1 Case study 56
4.2.2 Source and impact area 57
4.2.3 Hydrological model 58
4.2.4 Green-gray infrastructure scenarios 59
4.3. Results and discussion 62
4.3.1 Source and impact area identification 62
4.3.2 Comparison of effect difference 63
4.4. Conclusion 66
V. Conclusions 68
VI. Bibliography 70
Abstract in Korean 78

List of Figures

Fig. 1. Conceptual framework the research..5
Fig. 2. Study site location and land cover map (Seoul city, South Korea).....9
Fig 3. Data processing flow diagram and base maps in support of modeling 15
Fig. 4. Sensitivity test of four input variables for internal inflow on the (a) site I in 2010 and (b) site II in 2010 and (c) site I in 2011 and (d) site II in 2011 20
Fig. 5. Correlation between observed flood area and simulated flood volume for nodes on the (a) site I in 2010 and (b) site II in 2010 and 2011 22
Fig. 6. Hydrograph in 2010 flood event of (a) site I and (b) site II.............25
Fig. 7. Flood volume modeling results by enlargement percentage of conduit's cross- sectional area in 2010 flood event of (a) site I and (b) site II 26
Fig. 8. Research framework of the study 32
Fig. 9. Overview of the sewer network with DEM in the study area...........33
Fig. 10. Hyetographs of the design rainfall scenarios used in this study 34
Fig. 11. Changes in sewer network 39
Fig. 12. Conceptual framework for time-dependent UDS performance analysis (Song et al., 2019)...42
Fig. 13. Correlation between observed flood area and simulated flood volume for nodes in 2010, 2011 and 2013 43
Fig. 14. Hydrographs of the GI scenarios (S1~S4) under 20 rainfall events46
Fig. 15. Reduction rates of (a) peak flow rate and (b) runoff volume in the system for green infrastructure scenarios 47
Fig. 16. Flood hydrographs of the green-gray combination scenarios (S1~S6) under 20 rainfall events..48
Fig. 17. Reduction rates of flood volume in the system for green-gray infrastructure scenarios...49
Fig. 18. Changes in flood flow rate at the entire system between S1 and S6 50
Fig. 19. Research framework of the study 55
Fig. 20. Return period by duration time of 2010 flood event......................57
Fig. 21. Source and impact area derivation for green-gray infrastructure placement...63
Fig. 22.Flood hydrograph in 2010 flood event for S1~S4 and baseline 65
Fig. 23. Flood and runoff reduction rate by scenarios 66

List of Tables

Table 1. Observed precipitation value of flood inundation event 11
Table 2. Infiltration and surface flow volume before and after LID application 23
Table 3. Summary of GI characteristics 37
Table 4. Summary of areal statistics of GI application 38
Table 5. Overview of scenarios modeled in this study..............................40
Table 6. Precipitation data used for calibration...42
Table 7. Simulation parameters applied to SWMM model.......................44
Table 8. Resilience changes by flood events 50
Table 9. Precipitation data of flood inundation event 56
Table 10. Summary of GI characteristics 59
Table 11. Summary of green-gray infrastructure implementation 61
Table 12. Overview of scenarios modeled in this study............................62
Table 13. Overview of results by scenarios...64

Publications

Please note that some part of this dissertation proposal was written as stand-alone papers (see below), and therefore there is some repetition in the methods and results.

Bae, C., Lee, DK. Effects of low-impact development practices for flood events at the catchment scale in a highly developed urban area. International Journal of Disaster Risk Reduction, 44(101412).

I. Introduction

The frequency and magnitude of extreme rainfall are increasing because of urbanization and climate change (O'Donnell et al., 2019). Urban flooding negatively impacts infrastructure and humans and can lead to excessive damage costs (IPCC, 2014). Therefore, urban flood management (UFM) is essential for effectively managing the physical causes and potential effects of flooding by improving the structure and function of cities (Merz et al., 2010). The UFM ought to consider the connections and interactions between existing and new infrastructures to manage stormwater and improve the capacity to treat water (Vercrusse et al., 2019). Existing methods for treating water and mitigating urban flooding have focused on the volume expansion of sewerage systems. However, these measures are expensive and primarily aimed at water treatment, rendering them an unsustainable solution to unpredictable rainfall (Huang et al., 2020).

Thus, strategies have been proposed and applied over the past decade to control runoff and delay peak flow by restoring natural hydrological circulation and maximizing infiltration and retention capacities at sources (Palla et al., 2017). These strategies are expressed in various terms, including low impact development (LID), green infrastructure (GI), and nature-based solutions (NBS) (Ruangpan et al., 2020). Although each term has a different focus, it provides public benefits in addition to hydrological resilience, such as improved urban microclimate and biodiversity (Kuller et al., 2017). While the LID concept is for landscape functional-based storm care and GI is aimed at introducing ecological technology into existing infrastructure, NBS is a concept that has been frequently used since the 2010s to encompass existing concepts used regarding risk reduction (Nesshöver et al., 2017). This study used the GI concept, which integrates nature-based green and blue solutions and enhances and extends existing infrastructures (Dushkova and Haase, 2020). GI is a strategically planned network of natural and semi-natural areas, with other environmental features designed and managed to deliver a wide range of ecosystem services, such as water purification, climate change mitigation, and adaptation (Maes et al., 2015).

Various research methods, such as stochastic, empirical, probabilistic and deterministic methods, have been used to analyze the impact of urban flooding (Escuder-Bueno et al., 2012). Among them, deterministic methods using a hydrological model based on a simplified representation of the 'real world' are appropriate for identifying hazardous areas or confirming the effectiveness of spatial techniques such as green-gray infrastructures (Rodriguez et al., 2021).

Although several modeling researches has been conducted on the runoff mitigation effect of GI, most of these analyses have been conducted for building or block units. Few studies have identified the actual flood-mitigation impact based on parameter estimation and model updating at catchment-scale sites located at the boundary where rainwater is treated in an urban area. It is important to demonstrate strategies that can be implemented to reduce the flow at flooding sources and minimize flood risk at critical locations (Vleeschauwer et al., 2014; Fletcher et al., 2015; Dawson et al., 2020). Although the general theory of spatial impact is popular, modeling guidelines that can provide information for implementation in real-world plans are still lacking. In addition, few studies have tracked both grey-green infrastructure changes. Most studies were mainly based on surface and peak runoff reduction (Ercolani et al., 2018; Mei et al., 2018). Moreover, the impacts of the underlying rainfall patterns of GI on improving resilience are poorly understood. Urban flooding frequently occurs and has varying patterns; therefore, it is important to explore strategies for improving resilience and evaluating the efficiency of these strategies.

Research purpose reflecting these limitations of prior research are as follows. Chapter 2 tried to increase the accuracy of the results by constructing, calibrating, and verifying the urban flood simulation model based on the deterministic model. In addition, the effectiveness of GI as an adaptation strategy was evaluated. However, in Chapter 2, it was not tracking changes in the performance of green and gray infrastructure techniques. Furthermore, the effect of rainfall patterns, an important part of discussing resilience improvement, on the GI practices has not been analyzed. In consideration of these limitations, the performance of various rainfall patterns was analyzed in Chapter 3, and varying hypothetical performances by technology and sewage system changes were analyzed. In addition, by deriving resilience as well as runoff and flood volume, which are existing result indicators, the effect of green infrastructure was addressed by absorption and recovery concepts and analyzed. Chapter 4 attempted to conduct a modelling study based on the actual target site to prove the hypothesis that it is appropriate to install GI in the source area and to take structural protection measures in the impact area as summarized in previous studies.

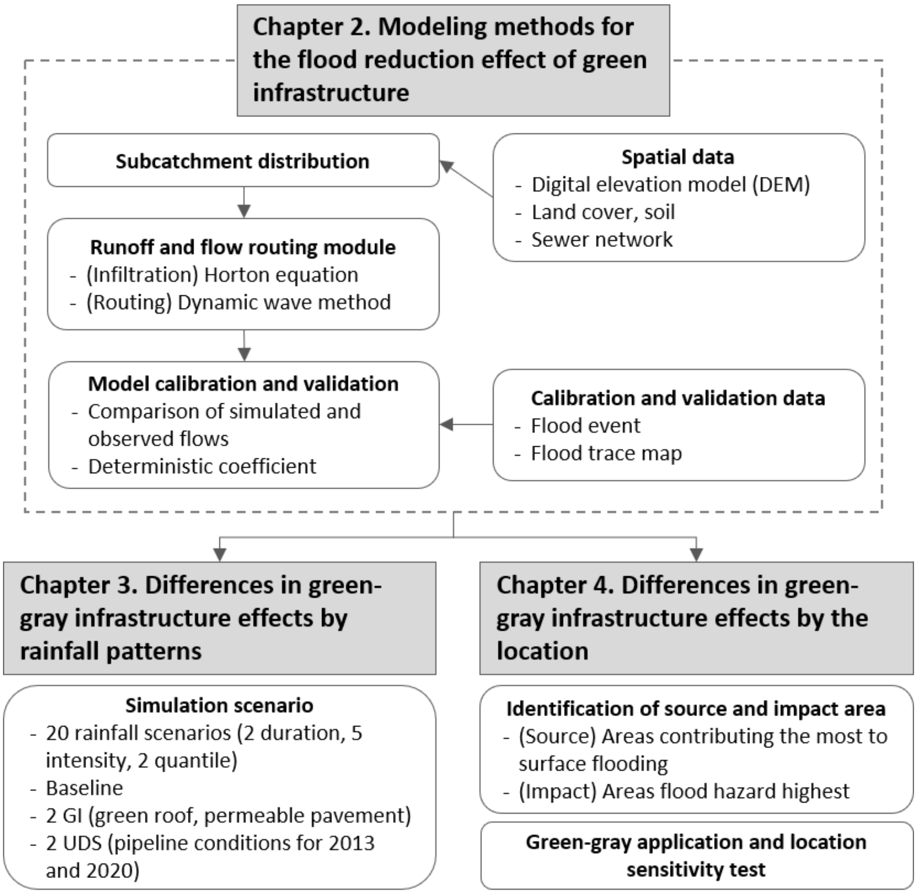

Fig. 1. Conceptual framework the research

II. Effects of low-impact development practices for flood events at the catchment scale in a highly developed urban area

2.1 Introduction

The frequency and magnitude of extreme weather and climate events such as heat stress, extreme precipitation, inland and coastal flooding, and water scarcity have been increasing steadily, posing risks to people, assets, economies, and ecosystems in urban areas (IPCC, 2014). Floods, particularly those in urban areas with a high percentage of impervious surfaces and high population density, can cause inundation of low-lying areas, which can result in indirect risks such as economic crises due to damage to electricity, gas, water supply, and transportation facilities (Yoon and Moon, 2009). In addition, projections of climate change associated with precipitation indicate the unpredictability of risks due to the low reliability of models and the spatially diverse and temporally dynamic patterns of hazards (IPCC, 2012).

According to statistics of major damage attributable to natural disasters in Korea over the past decade (2006–2015), the highest amounts of damage have been caused by heavy rains (63%) and typhoons (30%), which directly cause flooding (KMA, 2016). The Seoul metropolitan area, which is at risk of flooding due to its high percentage of impervious surface, has attempted to expand the sewer system and sewage pumping stations in response to frequent floods, but this has not been a sustainable solution for coping with climate change.

To address problems associated with urban water circulation, it is most cost-effective to consider water management during the planning phase. For this reason, various countries have proposed strategies for water management, such as green infrastructure, decentralized urban design, low- impact development (LID), and water-sensitive urban design. Different from conventional development patterns such as sewage concrete expansion, these strategies basically seek to reduce the impact of storm water runoff, restore and protect ecosystems, and retrench costs of constructing and maintaining storm water management infrastructure (Graham et al., 2003). Among these strategies, LID encompasses various strategies, such as rain gardens, green roofs, sidewalk storage, vegetated swales, buffer strips, rain barrels, and permeable pavement, and can be adapted to specific site characteristics (Prince George's County, 1999). The effects of LID on runoff have been studied in various scales (Inkiläinen et al., 2013; Palla et al., 2017), as well as by the design elements of the individual LID practices (Montalto et al., 2007; Diezt, 2007). Recently, the effectiveness of LID has also been highlighted as a potential option to reduce urban flood risks (Ellis, 2012; Kim et al., 2016). While the installation of storage facilities is mainly proposed as a flood reduction option, there is a limitation in that new spaces for large-scale facilities cannot be allocated in highly developed urban areas (Duan et al., 2016). This study intended to apply LID for urban retrofitting in small spaces, such as parking lots, sidewalks, and buildings.

In addition, although much modeling research has been carried out on the runoff mitigation effect of LID, most of these analyses have been conducted for building or block units, and few studies have identified the actual flood-mitigation impact based on parameter estimation and model updating at a catchment-scale site located at the boundary where rainwater is treated in an urban area.

The main objective of this study was to identify the hydrological benefits of urban disaster prevention by LID using a simulation model. Under these objectives, practical LID was applied to the catchment scale to derive realistic disaster risk reduction at the study site, and flood events were applied and verified. The identification process consisted of four main components: (1) site analysis and simulation model configuration, (2) design criteria setting of applicable LID practices, (3) model updating through sensitivity testing and parameter estimation, (4) impact analysis of LID practices on flood events.

2.2 Methods

2.2.1 Study site

2.2.1.1 Spatial data

The study site was located in Seoul, the capital of South Korea, one of the most densely populated cities worldwide. The extensive urbanization of Seoul in the 1960s and 1970s led to rapid expansion of the city without appropriate definition or consideration of terrain characteristics and flooding in the urban development process (Koh and Lee, 2012).

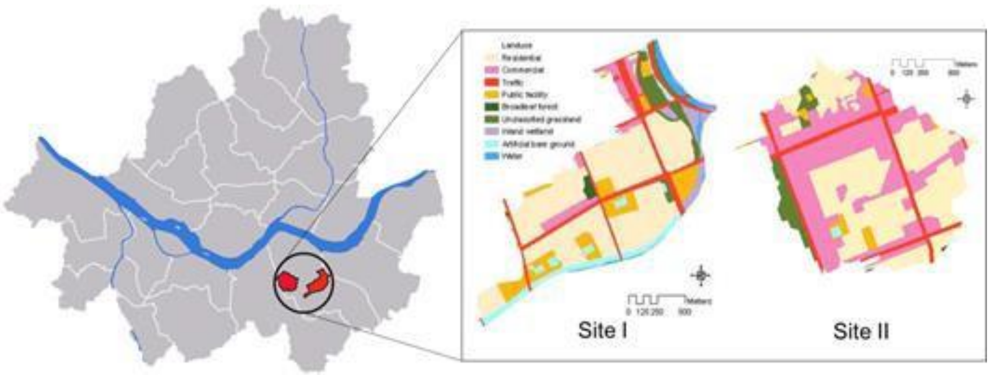

Fig. 2. Study site location and land cover map (Seoul city, South Korea)

In this study, two case sites were selected at the catchment scale, which represents the basic scale for determining the amount of domestic water in urban areas and minimizing other impacts. The first case site (site I) within Seoul city is a typical densely built and highly populated residential catchment-scale sector with a low amount of green space. The 198.89-ha case site located at an elevation of 5–44 m is bounded by a tributary to the Han River, and more than 80% of the total area is impermeable, which means that it can be regarded as a high-density lowland development area. The second case site (site II), adjacent to site I, is a typical commercial area with an area of 192.61 ha, elevation of 14–71 m, and an impermeable area of 85%. Both case sites have a history of flooding, in 1984, 1990, 1998, 2001, and then again in 2010, despite sewer construction. Fig. 2 provides an overview of the study sites.

2.2.1.2 Meteorological data

In modeling studies, it is common practice to use probable rainfall data; however, in this study, rainfall events that caused actual flooding were applied as meteorological data because the model was updated through parameter estimation using actual rainfall events as the basis for correction.

The observation data of precipitation were collected at the automated weather station (AWS) of Gangnam (37.5131° N, 127.0470° E), which is the nearest rain gauge to the case sites. The rainfall data from the AWS were measured with a resolution of 5 min.

The Asia-monsoon, also called the seasonal wind, is associated with intense rainfall and are typically generated by seasonal changes in wind and atmospheric pressure. The Korean peninsula is mainly affected by the North Pacific High in summer, and more than 50% of the annual precipitation is concentrated within the monsoon season (Seo et al., 2011). The monsoon season in Korea is concentrated in July and August, and the flood event selected in this study also corresponds to this period.

The 2010 rainfall event had a relatively short duration, but the hourly maximum rainfall was 71.0 mm/h, which is close the 10-year return period of 1-h duration precipitation calculated for Seoul of 73.6 mm/h (MLTM, 2011). In 2011, the rainfall intensity was lower than in 2010, but the rainfall lasted for 30 hours without sufficient drainage time (See Table 1). These two flood events caused a maximum of 1 m of water to flow into the streets of the city, temporarily stopping traffic. According to national statistics, the property damage in Seoul, including the loss of roads and the flooding of houses, in 2010 and 2011 was estimated to be 14.5 and 75.9 million USD, respectively (KMA, 2010; KMA, 2011).

Table 1. Observed precipitation value of flood inundation event

Rainfall events	Duration time	Sum of precipitation	Maximum hourly precipitation
2010.09.21. 08:00 - 22:00	14-hr	292.5 mm	71.0 mm
2011.07.27. 15:40- 2011.07.28. 22:40	30-hr	414.5 mm	58.0 mm

2.2.2 Urban rainfall-runoff modeling

2.2.2.1 Storm Water Management Model

The growing importance of flood risks for cities has led to an interest in rainfall runoff modeling, which is the primary tool used to simulate runoff quantity and quality from changes in rainfall and land use. Modeling provides information about the efficiency of a system before applying the best system to achieve the intended goal. Numerical rainfall–runoff models capable of representing spatiotemporal variations have been developed (Singh and Woolhiser, 2002). In this study, the Storm Water Management Model (SWMM) ver. 5.0 was selected as a model capable of analyzing LID practices while also considering sewer system flow routing and overflow structures (Duan et al., 2016; Rossman, 2010). SWMM, developed in 1971 by the U.S. Environmental Protection Agency, is applicable to both continuous and single rainfall events. It also has the advantage of being able to analyze various time steps of rainfall. For instance, Bhaduri et al. (2001) used SWMM to analyze the potential hydrological impacts of land-use changes, and Tsihrintzis and Hamid (1998) applied the model to predict runoff quality in a small urban watershed. Furthermore, studies related to the calibration and verification for enhancing model reliability (e.g., sensitivity test parameters and comparison of various study sites) have made major advances (Warwick and Tadepalli, 1991). SWMM is calculated by four subroutine blocks with unique features, where the results are saved and used as the inputs for other blocks (Huber and Dickinson, 1988). The EXECUTIVE block sets the file and logical device, transfers data between blocks, and outputs the operation result. The RUNOFF block, a simplified drainage catchment, is the first model operation that simulates the runoff from the drainage catchment for a rainfall event, and it provides a hydrograph that is used as the basic data by the other blocks. The non-linear reservoir method is applied to the runoff calculation of this block using Manning's formula and the continuity equation (Dooge, 1973). The TRANSPORT block tracks the flow rate in the sewer system in the dry or wet season based on the values calculated from the RUNOFF block. The calculation of the outflow from this block uses the kinematic wave routing technique.

2.2.2.2 Model configuration

The subcatchment is mainly divided using a topographic map and sewer networks considering the locations of the main maintenance holes and conduits. First, for runoff analysis through SWMM, it is necessary to construct the input data and processing parameters. Parameters related to runoff can be largely classified into hydrological and physical parameters

(Huber and Disckinson, 1988). Hydrological parameters include the roughness coefficient and the depression storage of pervious or impervious areas and conduits. Physical parameters include the subcatchment, impervious areas, and the shapes of conduits. These parameters should be considered when simulating urban runoff, but it is difficult to determine all parameters accurately. Therefore, some parameters should be estimated within the range suggested in previous studies, considering the site characteristics.

Physical parameters are variables that can be understood through basic analysis using ArcGIS ver. 9.3, as shown in Fig. 3. The conduit includes all closed rectangular and circular conduits with diameters of more than 1000 mm for the main sewer. The shape, length, and depth of each conduit are listed with reference to the sewer network map. Because surface runoff is assumed to flow perpendicularly to the conceptualized rectangular catchment in SWMM, the width of the subcatchment is calculated by dividing the area by the length of the drain pipe. This parameter may include uncertainty because the actual subcatchment is not a rectangle, contrary to the assumption. The digital elevation model and average slope are calculated using a topographic map divided into subcatchments. The impervious area ratio is calculated using an urban biotope map. LID is analyzable by defining a new space in each subcatchment.

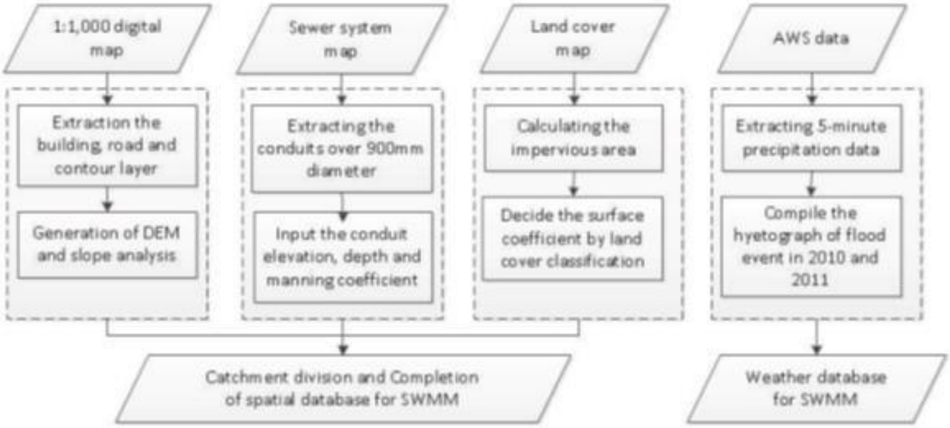

Fig 3. Data processing flow diagram and base maps in support of modeling

The main hydrological parameters in this study were curve number (CN) value, depression storage, and Manning's roughness coefficient. Among several methods for calculating infiltration rate, this study applied the runoff CN method of the Soil Conservation Service developed in 1972. The CN has a value from 0 to 100 that is determined by land use, hydrological soil group, and cover type. In addition, the antecedent moisture condition (AMC) is used to represent the watershed's potential runoff before rain occurs. The AMC is classified into AMC-I, -II, and -III. The CN value is adjusted to the antecedent rainfall of 5 days. In the rainfall events used in this study, the AMC-III phase was continuously applicable, except for the first several hours. The concept of depression storage depth assumes that surface runoff does not occur before the surface is sufficiently stored (wetted) in pervious or impervious areas.

Water loss occurs by infiltration and evaporation in permeable areas, but it occurs by only evaporation in impervious areas. The roughness coefficient of the surface is not specifically classified because there are substantial changes caused by land cover. Nevertheless, Engman (1986) analyzed the range of the estimated values calculated by the kinematic wave formula based on measured rainfall runoff data. Thus, we attempted to investigate the parameters sensitive to the output value within the range of depression storage depth suggested by the ASCE (1982) and Manning's roughness coefficient defined by Engman (1986).

2.2.3 Low-impact development

The Ministry of the Environment in Korea proposed applying LID practices to major development plans in 2013, and there have been many studies on LID practices applicable to urban areas and hydrological functions according to their design elements. Such studies have shown that green roofs and permeable pavers are appropriate, and effectively reduce the potential for runoff in highly developed residential urban areas.

Green roofs effectively delay peak runoff and lower roof temperature via evapotranspiration through soil and vegetation (Dietz, 2007). As a result of research conducted on the hydrological functions of green roofs, VanWoert et al. (2005) reported that factors such as slope and media depth must be considered if the objective is to maximize rainfall retention. Furthermore, Dunnett and Kingsbury (2004) proved that the substrate depth, roof slope, plant community type, and rainfall pattern affect the runoff rate. The magnitude of retention depends on the substrate depths of the various layers (Montalto et al., 2007; Mentens et al., 2006). In a review article, Dietz (2007) explained that soil depth is the most important factor of green roofs for reducing rainwater runoff. Green roofs basically consist of vegetation, substrate, and drainage layers (Mentens et al., 2006), and are generally divided into two types: intensive and extensive types. Intensive green roofs are able to incorporate all sizes and types of vegetation based on a deep substrate of more than 150 mm (Obermdprfer et al., 2007). Extensive green roofs generally have a shallower substrate layer of approximately 150 mm and require less maintenance than intensive roofs, but can accommodate only a limited range of vegetation species (Dunnett and Kingsbury, 2004).

Permeable pavements are typically made of a matrix of concrete blocks that includes voids filled with sand, gravel, or soil. These voids allow runoff to infiltrate through the pavement into the underlying soil, mitigating the impact of runoff and recharging groundwater (Brattebo and Booth, 2003; Lee et al., 2001). Because dust or particulate matter emitted from automobiles can reduce permeability over time, it is suitable to install permeable pavement in spaces such as parking lots, driveways, and road shoulders, where traffic volume is low and maintenance management is easy (Brattebo and Booth, 2003; Shackel et al., 2003).

In this study, two interviews of experts were conducted to consider the characteristics of buildings in Korea and the workability and maintenance of green roofs. As a result, extensive green roofs were selected and soil depth, which is an important factor, was set at 200 mm. Slopes were applied at a minimum rate of 2%, which is specified in the 2012 design standard, and porosity was set to 50% considering the soil material that is usually used.

In the case of permeable pavement, studies have described limitations in addressing maintenance problems, so only roads with apartments complexes and parking spaces with less traffic than general roads were set as target areas. An 80-cm-thick (surface 20 cm, base 30 cm, sub-base 30 cm) permeable pavement, which yields the largest runoff reduction based on an analysis by Lee et al. (2001) and Shackel et al. (2003), was applied in this study.

Parameters not considered in the expert interviews and literature review were set to the default values of the model.

The spaces where green roofs and permeable pavement could be installed were extracted from public buildings and apartments, and impervious parking spaces and roads in apartment complexes using 1:1,000 digital topographic maps; areas where these measures were already installed were excluded. The maximum applicable area for green roofs was about 22.34 ha at site I and 27.61 ha at site II, 11.7% and 14.3% of the total areas, respectively. Site II did not meet the criteria for installing permeable pavement, and only 6.98 ha (3.0%) of site I was suitable for permeable pavement installation.

2.3 Results and discussion

2.3.1 Model updating

To improve model reliability, two processes were attempted in this study: (1) sensitivity testing to derive input variables that affect results and (2) model updating by estimating the input values based on the flood inundation map.

As shown in Fig. 4(a and b), the sensitivity test was performed on four input variables (depression storage of impervious/pervious surface and Manning's N value of impervious/pervious surface, respectively) within a specific range, not a fixed value. The variation of the simulated overflow value was observed by changing the x-axis from 10% to 50% based on the four input variables. Manning's N value of pervious surface was most sensitive at site I, and Manning's N value of impervious surface was most sensitive at site II. However, the degree of sensitivity to variable adjustments depended on the site and the rainfall event. Depression storage affected overflow similarly in all cases.

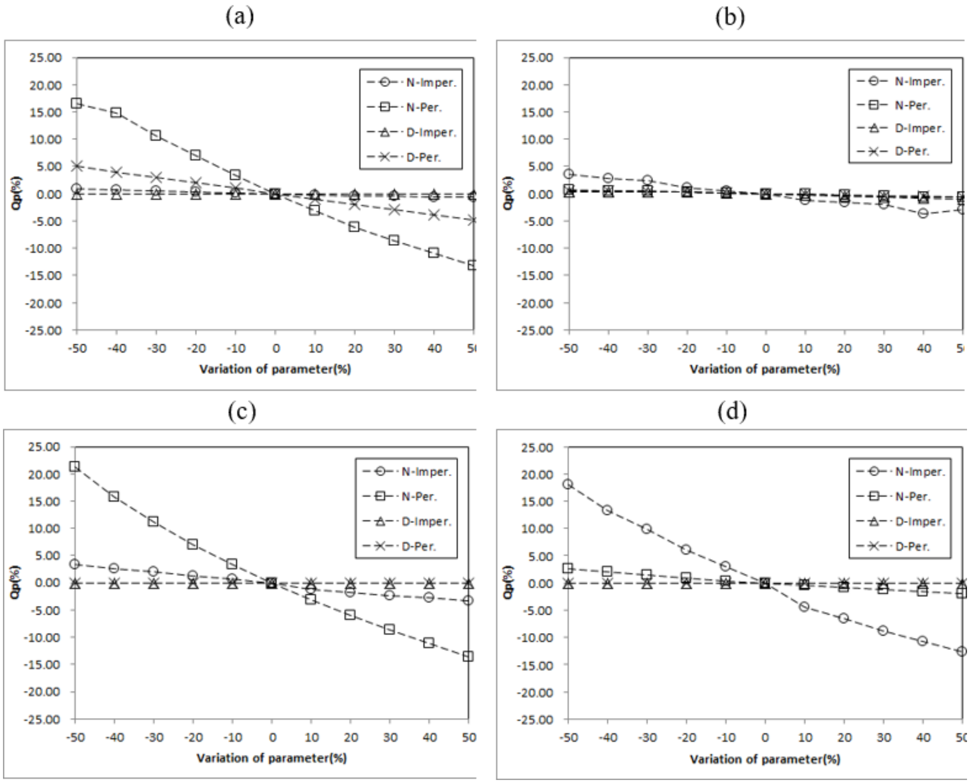

Fig. 4. Sensitivity test of four input variables for internal inflow on the (a) site I in 2010 and (b) site II in 2010 and (c) site I in 2011 and (d) site II in 2011

Most studies on this subject did not make near-real-time corrections because the rainfall data were based on the probability rainfall distribution. However, in this study, we set the spatiotemporal data based on the actual rainfall events in a catchment-scale area in which actual outflow occurs.

Nevertheless, because the model updated based on the results of the sensitivity test for single parameters, we could not consider the land cover characteristics of the urban area, which are becoming more diverse, or the variability of rainfall patterns. Recent studies have noted that not only the main parameters but also the accuracy of the calibration may vary depending on parameter interactions (Jato-Espino et al., 2017). In future research, it will be necessary to clarify the interactions among parameters based on changes in rainfall patterns and land cover data and then re-identify the main parameters. Finally, automatic calibration to search the optimized combination of parameters will increase the modeling accuracy.

In the next step, the most sensitive input values were adjusted for each site within the respective range to approximate the inundated area based on the flood inundation map. The updated simulation results from the repeated execution of the variable adjustments showed accordance with the points (nodes 02, 05, 06, and 11 at site I in 2010; node 01 at site I in 2011; nodes 02, 04, 06, 12, 13, and 15 at site II in 2010; and nodes 02, 04, 06, 12, 13, and 15 at site II in 2011) where overflow occurred on the flood inundation map.

Because the flood inundation map used in this study presented only information about the location and area, comparison with the volume-based simulation results was limited. However, assuming that the flood depth is almost constant and that the elevations of the locations where flood inundation occurred at each site were similar, the updated simulation results showed high correlation with the observation data (Fig. 5(a and b)).

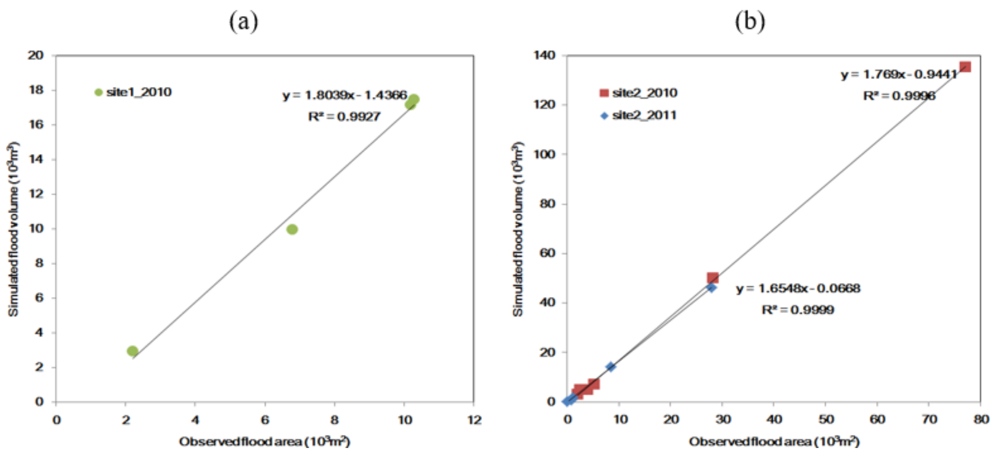

Fig. 5. Correlation between observed flood area and simulated flood volume for nodes on the (a) site I in 2010 and (b) site II in 2010 and 2011

It is expected that a more accurate verification process could be carried out if data providing information about flood volume (e.g., water level in maintenance holes, flood depth) were accumulated by the local government.

2.3.2 Effects of LID practices on flood events

The results were divided into two cases: (1) conventional sites (no LID) and (2) LID-applied sites (LID). The runoff and flood volume for the entire study area were determined for both cases. Table 2 shows the volume derived from the modeling results. Overall, runoff and flood volume decreased slightly and infiltration volume increased after application of LID. In particular, flood volume in site I was reduced to 54.6%. The flood event in 2011 showed a significant increase in infiltration because of rainfall over a long period of time; site II, which had a relatively large impervious area ratio, showed a larger increase in infiltration after LID installation. Overall, LID did not affect the occurrence of flooding, but the flood reduction effect was 2–5 times greater than that of runoff.

Table 2. Infiltration and surface flow volume before and after LID application

Rainfall event	Components	site I			site II		
		No LID	LID	Reduction (%)	No LID	LID	Reduction (%)
2010. 9.21.	Infiltration (10^6L)	15.0	39.4	-163.1	1.6	26.2	-1,576.3
	Runoff (10^6L)	507.5	445.7	12.2	540.9	482.2	10.9
	Peak runoff (CMS)	46.5	45.0	4.0	52.3	51.1	2.2
	Flood (10^6 L)	47.5	21.5	54.6	205.0	154.3	24.8
	Outflow (10^6 L)	472.8	427.6	9.6	338.3	330.2	2.4
2011. 7.27-28.	Infiltration (10^6 L)	15.2	79.1	-419.5	1.6	62.5	-3,848.1
	Runoff (10^6 L)	757.3	653.7	13.7	799.5	699.2	12.6
	Peak runoff (CMS)	33.8	29.3	13.5	53.2	46.6	12.3
	Flood (10^6 L)	5.8	3.0	48.4	63.2	36.5	42.3
	Outflow (10^6 L)	743.8	644.2	13.4	743.6	666.1	10.4

In addition, this study compared the effect of pipe extension to analyze the performance of LID practices on flood events. The flood events in 2011 resulted in a less-flooded condition at site I than those in 2010; therefore, we examined only the effects on the events of 2010.

Fig. 6 shows a hydrograph of the runoff and flood volumes before and after LID application based on the modeling results for the 2010 rainfall event. Here, runoff refers to a continuous surface runoff from the subcatchments, and node flooding occurs when a pipe is under pressure due to a large amount of runoff, which means the water rises and inundates in a small vertical tube connected to the pipe. At site I, there was no delay in the runoff start time, but the effect of the flood start time delay was confirmed to be 55 minutes. At site II, the flood start time was not delayed because the sewer network did not treat the instantaneous high rainfall intensity, but the initial flood amount was reduced by 67%.

(a)

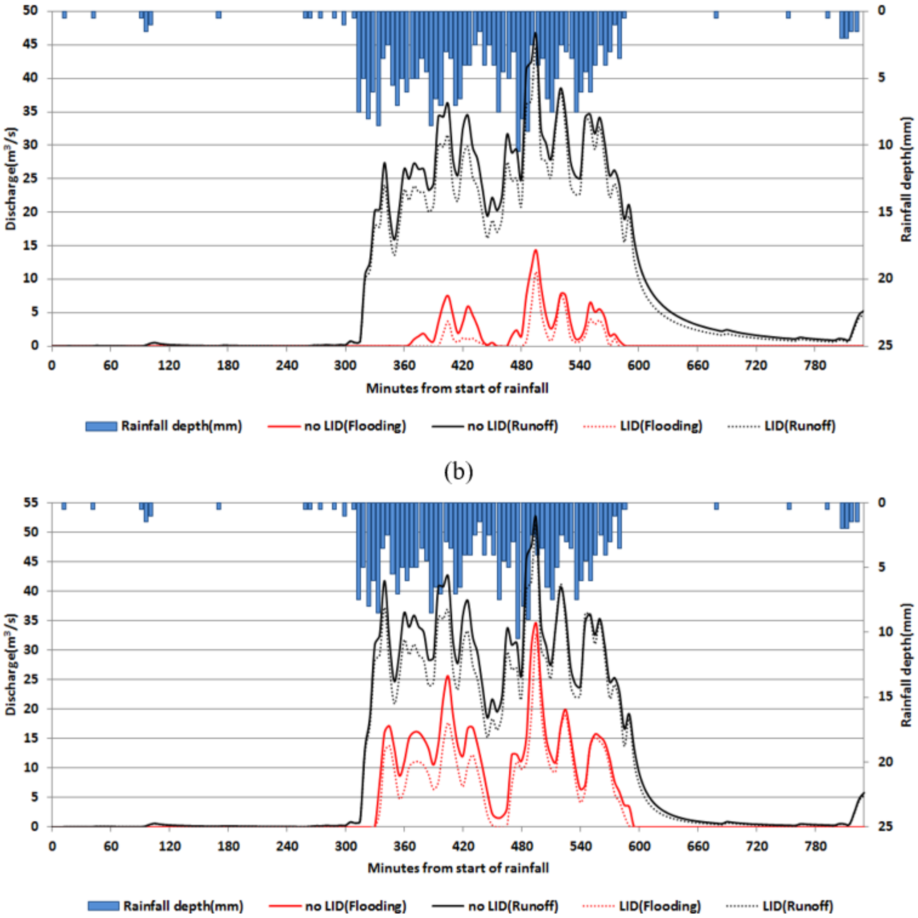

Fig. 6. Hydrograph in 2010 flood event of (a) site I and (b) site II

To compare the effect of LID with pipe extension, the flood volume was modeled by enlarging the percentage of conventional conduit cross-sectional area at the entire site for both cases before and after LID application (Fig. 7). At site I, LID application had the same effect as an 11% conduit enlargement; at site II, it had the same effect as a 13% conduit enlargement.

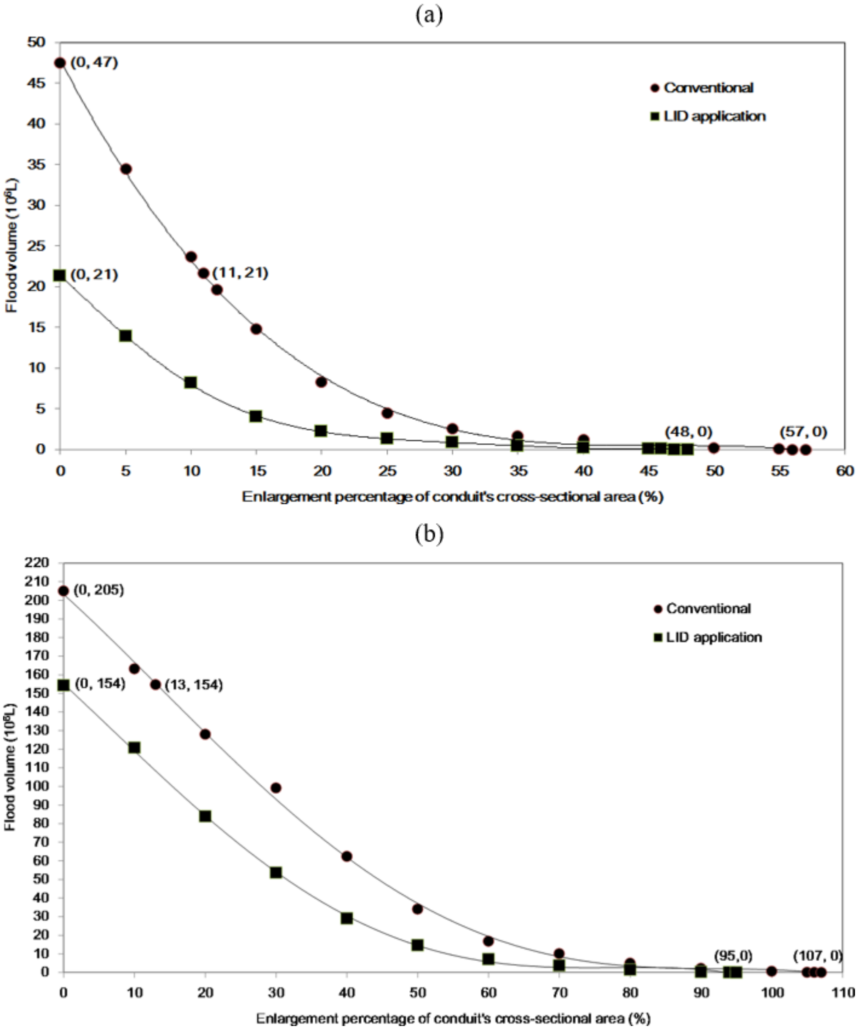

Fig. 7. Flood volume modeling results by enlargement percentage of conduit's cross- sectional area in 2010 flood event of (a) site I and (b) site II

2.4 Conclusions

To quantitatively evaluate the effects of LID practices on flood mitigation, we modeled study sites in Seoul using SWMM based on current land use and sewerage arrangements. Both the selected storm water runoff model and LID practices were evaluated based on theoretical considerations, previous research, and expert advice. To exclude impacts other than those from LID practices, the study site was set as a catchment-scale site with an independent drain system and drainage sector organized by one outfall. In addition, this study attempted to improve the accuracy of the simulation result by model updating based on sensitivity testing and parameter estimation based on actual rainfall events that caused flooding.

Parameter sensitivity differed depending on the impervious ratio of the site or rainfall characteristics. In this study, depression storage was not a sensitive parameter, but surface roughness was. In all cases, applying LID practices reduced runoff and flood volume and enhanced infiltration and surface storage. LID did not affect the occurrence of flooding, but the flood reduction effect was 2–5 times higher than that of the runoff. The results showed that the same effect could be obtained by enlarging the conduit cross-sectional area of the whole site by 11–13%. Although large-scale LID applications, such as storage facilities, may have a noticeable hydrological effect, most highly developed urban areas do not have sufficient space for such facilities. The methodology of this study can be used to assess the performance of the LID practice when establishing urban regeneration or redevelopment plans for saturated urban areas.

However, this study has some critical limitations. First, the calibration was not ideal because the model was updated based on the sensitivity testing of a single parameter and because only two flood events were analyzed in the case study. In addition, flood monitoring was not carried out at the national level, and the output data for calibration were not exact. In conclusion, because the calibration process of this study clearly demonstrates that LID performance is affected by rainfall pattern and land surface, future research should explore a methodology that can be used to evaluate these considerations.

III. Quantifying the effect of green-gray infrastructure at the catchment scale under various rainfall patterns

3.1. Introduction

Floods have been one of the most frequent global natural disasters in recent years (Wang et al., 2019). In particular, urban flooding causes widespread human casualties and considerable economic losses. Therefore, it is important to develop response strategies to these events (Arjenaki et al., 2021). The installation of drainage systems is a conventional response strategy that is designed using a deterministic approach based on catchment properties and storm design. This approach links to the purpose of drainage system on managing site runoff and promptly storing the runoff in drainage facilities (Yazdanfar and Sharma, 2020). However, as recent trends in climate change have led to more frequent and highly variable rainfall events, urban drainage systems (UDSs) designed using a deterministic approach are often threatened. Thus, the need to build resilience into UDSs is increasingly recognized as a means to ensure that these systems are able to adapt to highly uncertain threats (Mugume et al., 2015).

Resilience means to endure and maintain function and structure after a disturbance event (Davoudi et al., 2012). Urban resilience is the ability to withstand disasters through absorption, recovery, and adaptation (Folke, 2006). It is known that adjusting social-ecological systems contributes to absorbing adverse effects (Cosens et al., 2013). Since urban flooding occurs frequently and haphazardly, it is important to investigate strategies for improving resilience and evaluating their efficiency (Li et al., 2016).

During the past decade, green infrastructure (GI) strategies have been proposed and implemented as alternatives to conventional gray infrastructure strategies, such as drainage systems. GI strategies control and delay the peak flow of runoff by restoring natural hydrological circulation and maximizing the infiltration and retention capacities at source (Eckart et al., 2017; Qin et al., 2018). Research on the effects of GI implementation mainly comprises impact assessment studies that are based on applying GI practices. For example, Qin et al. (2018) analyzed the effects of applying permeable pavements (PPs) and green roofs (GRs) under various rainfall patterns, and Tao et al. (2017) also found that GI practices are less effective in high-intensity storm scenarios. Many studies evaluate performance changes when applying GI practices, but few studies simultaneously track changes in the performance of green and gray infrastructure techniques. Furthermore, most studies are based on the results of reducing the surface and peak flow of runoff (Ercolani et al., 2018; Mei et al., 2018). In addition, there is a gap in our understanding of the underlying impacts of rainfall patterns on the GI practices used for improving resilience.

Therefore, this study attempted to clarify the interaction between GI practices and urban drainage system (UDS) outflow based on simulations that underwent calibration using the GI concept. Simulation and modeling applications are the most commonly used applications, which are suitable to provide information that supports decision-making when evaluating the performance of systems and potential changes in conditions from baseline scenarios or planned outcomes (Jia et al., 2015). This study conducts the following research to investigate the effects of GI implementation on urban flooding: 1) Investigates the effects of GI implementation under various rainfall patterns and the changes in UDSs and 2) elucidates how these effects can be interpreted in terms of resilience.

The investigation aims to evaluate the effects of the most commonly used GI practices, such as GRs and PPs, at the urban catchment scale. This includes the impact of the implemented GI practices on changes in drainage systems. Urban planners need to understand to what extent the structure of existing sewerage systems is affected when the combined effects of GI implementation and gray infrastructure improvements are considered. This study assesses the effectiveness of the sewerage network without simplifying or modifying it. In addition, analyzing various rainfall patterns will enrich our awareness and knowledge regarding the actual effects of implementing GI practices. The research framework is presented in Fig. 8.

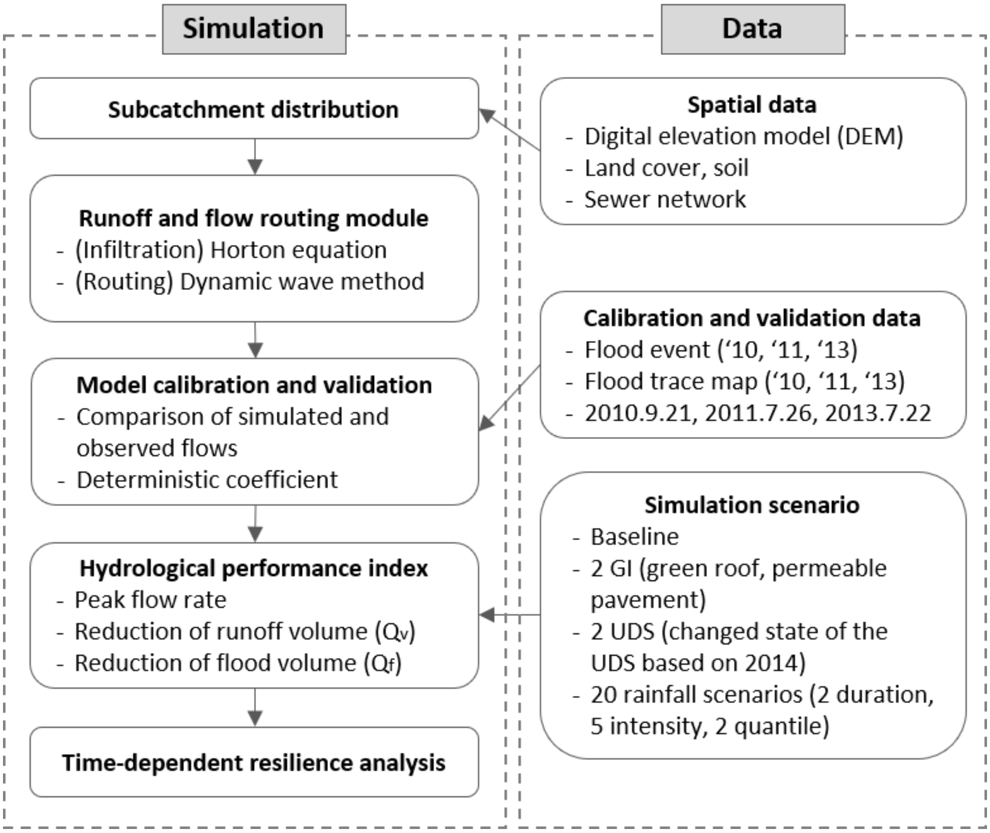

Fig. 8. Research framework of the study

3.2. Materials and Methods

3.2.1 Case study

Large cities in East Asia are vulnerable to flood risks due to climate change and high urban development density (KMA, 2020). In this study, the "catchment scale," which is the basic scale for water resource planning (such as determining the size of water maintenance in urban watersheds), was set as a spatial scope (Fig. 9). In addition, the study target area was the Yeoksam-dong commercial area (192 ha) in Seoul, a high-density city. Although several floods occurred around the 2000s in Seoul, the UDS was upgraded, and flooding occurred afterward; therefore, it is suitable to compare the effects between the GI practices and the improvement in UDSs.

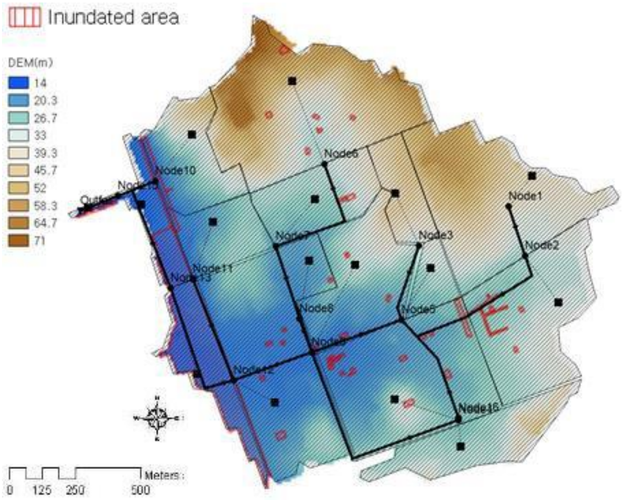

Fig. 9. Overview of the sewer network with DEM in the study area

3.2.2 Applied meteorological data

This study used design rainfall to investigate the response of the surface and pipe networks in various rainfall patterns. This is suitable for contrast analysis according to the green-gray infrastructure control conditions.

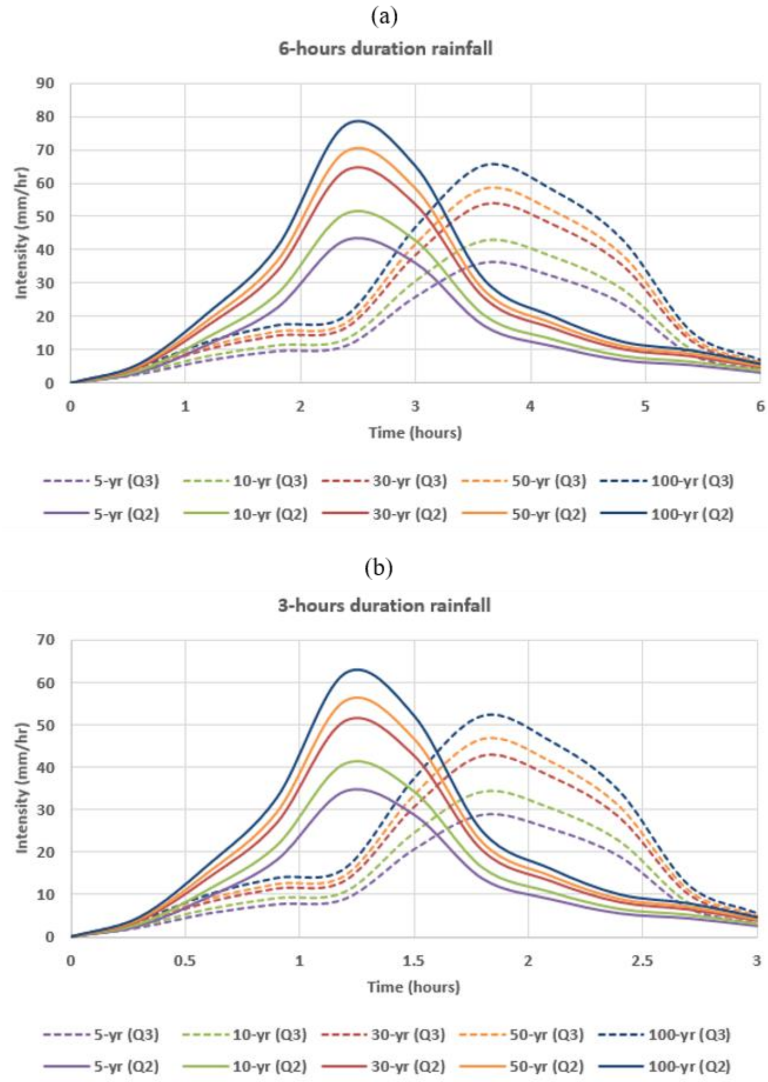

Fig. 10. Hyetographs of the design rainfall scenarios used in this study

Probability rainfall data for the study target area provided by ministry of environment (MOE) (2019) were used, and time was distributed using the method of Huff (1967). Huff (1967) shows in which section the maximum amount of rainfall occurs by duration. The rainfall duration is divided into four quartiles using the rainfall mass curve as screening data for each duration. In this study, through previous studies, the 3rd-quartile derived from the time distribution that appeared the most in South Korea was selected (Park et al., 2018), and the 2nd-quartile was additionally selected to compare it with the 3rd-quartile.

In this study, 20 rainfall events were selected with 5 return periods (5-years, 10-years, 30-years, 50-years, 100-years), 2 durations (3-hour, 6-hour), and 2 types of time distributions (2nd-quartile, 3rd-quartile). The calculated synthetic hyetographs of all events in this study are shown in Fig. 10.

3.2.3 Hydrological assessment

This study used the stormwater management model version 5.1 (SWMM v5.1) (hereinafter referred to as SWMM) for the hydrological assessment. The SWMM is a physical process-based discrete-time simulation model that considers sewerage flows in cities for hydrological analysis and facilitates the application of natural-based technologies such as GI practices (Rossman, 2010). All hydrodynamic analyses were performed based on the sewerage network implemented by Bae et al. (2020). This model includes 16 sub-catchments that drain into 16 junction nodes connected to 15 conduit links.

Infiltration refers to the process by which rainfall is absorbed into the underground surface and perforates into unsaturated soil layers. The Horton method was used in the model. Surface runoff occurs when the maximum infiltration capacity is exceeded. Manning's equation was applied to the runoff volumes, and the flow routing was based on the dynamic wave theory. Antecedent moisture conditions (AMC), which are an indicator of the moisture of the catchment, provide a representation of soil moisture storage 5 days prior to rainfall event; this indicator has been is applied in the AMC-III step in this study.

A hydrological performance index can evaluate the effects of different scenarios. Previous studies that analyzed the GI implementation effects of small catchments were reviewed (Damodaram et al., 2010; Ercolani et al., 2018). The peak flow rate (m^3/s), the reduction rate of runoff volume (Qv, m^3), and the flood volume (Qf, m^3) values were selected as outputs of the simulation summary in the SWMM. Here, the peak flow rate refers to the highest flow rate of the outflow system, runoff volume refers to the volume of water that runs off the target site from a prescribed storm event, and flood volume refers to the volume exceeding the channel capacity (Mei et al., 2018).

3.2.4 Green-gray infrastructure

In this study, two GI techniques were considered: GRs and PPs. GRs mainly provide infiltration and evaporation, while PPs act as temporary water storage facilities before stored water is discharged from the underground drain to the lower watershed outlet.

In the SWMM, the GI practices were expressed using a combination of vertical layers of surface, soil, and storage, and the design elements for each were applied using the parameters suggested in previous studies (Rodriguez et al., 2021; Abualfaraj et al., 2018; Tirpak et al., 2021; Randall et al., 2019).

Table 3. Summary of GI characteristics

	Parameter	**Permeable pavement**	**Green roof**
Surface	Bern height [mm]	5	75
	Vegetation volume fraction	0	0.1
	Roughness (Mannings n)	0.05	0.1
	Slope	2	0.3
Soil/Sand	Thickness [mm]	-	150
	Porosity	-	0.4
	Field capacity	-	0.105
	Wilting point	-	0.047
	Conductivity [mm/hr]	-	72
	Suction head [mm]	-	20
Pavement	Thickness	150	-
	Void ratio	0.4	-
	Impervious surface fraction	0.3	-
	Permeability [mm/h]	72	-
Storage / Drainage mat	Thickness [mm]	150	50
	Void fraction	0.5	0.55
	Seepage rate [mm/hr]	78	-
	Roughness (Mannings n)	-	0.3

In this study, the type and location of GI practices were primarily determined by the land cover characteristics of the research area. For the land cover of the target study area, GRs were designed for all residential, administrative, and commercial buildings, while PPs were implemented for walkways in traffic areas. A statistical summary of the GI practices applied for sub-catchments is shown in Table 4.

Table 4. Summary of areal statistics of GI application

Subcatchment number	Total area (ha)	Green roof application area (ha)	Permeable pavement application area (ha)
0	10.4	1.7	0.1
2	23.0	3.8	0.9
3	8.0	1.7	0.3
4	24.3	7.1	0.7
5	3.4	0.7	0.2
6	3.3	0.4	0.1
7	18.2	2.3	0.4
8	0.2	-	0.1
9	6.5	0.9	0.2
10	14.0	1.6	0.2
11	9.4	1.1	0.3
12	5.4	0.5	0.3
13	5.2	0.2	0.2
14	23.5	2.5	0.9
15	9.7	0.5	0.1
16	28.0	2.5	0.9
Sum	192.5	27.5	5.9

The changes in the gray infrastructure focused on the changes in the sewerage pipeline network. The target study area is known for frequent flooding; thus, the expansion and extension of sewerage pipes has been highlighted at several instances. In this study, two scenarios signified the state of the UDS. The former scenario (UDS1) and the latter scenario (UDS2) were based on 2014, a date after the 2010, 2011, and 2013, which was used for calibration. The changes in the UDS at the target study area are presented in Fig. 11, and the blue-marked UDS shows the newly constructed conduit, including the gray-marked UDS1.

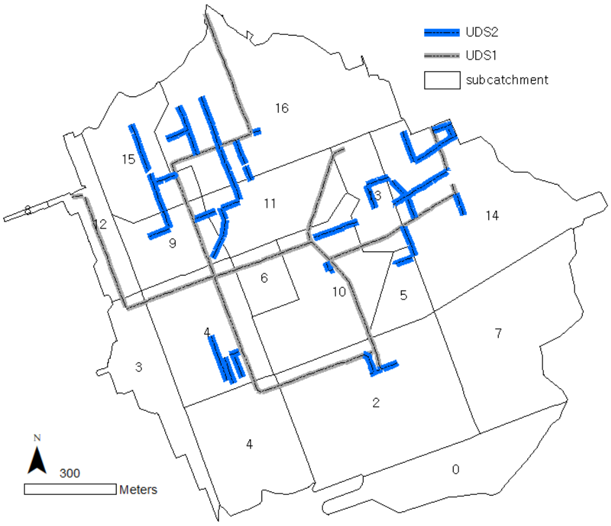

Fig. 11. Changes in sewer network

The scenarios signifying the changes in the implementation of green-gray infrastructure were divided into 6 cases, which included a baseline case (S1) that represented no infrastructure implementation (Table 5).

Table 5. Overview of scenarios modeled in this study

Scenario	Combination		
	GR (ha)	**PP (ha)**	**UDS**
S1: Baseline (no-GI, UDS1)			1
S2: UDS1+GR	53.8		1
S3: UDS1+PP		5.9	1
S4: UDS1+GR+PP	53.8	5.9	1
S5: UDS2			2
S6: UDS2+GR+PP	53.8	5.9	2

3.2.5 Time-dependent resilience assessment

There are several studies highlighting resilience to urban floods. The definition of urban flood resilience, as proposed in previous studies, largely makes notion of 1) the ability to recover after stress and 2) the ability of the group to cope with external stress (Leandro et al., 2020). Bertilsson et al. (2019) developed an indicator-based resilience evaluation framework in consideration of resistance and recovery, and attempted mapping scenarios signifying the pre- and post-introduction periods of adaptation strategies. Wang et al. (2019a) derived changes according to the retrofitting options scenario using a resilience graph based on volumetric output. Wang et al. (2019b) has derived severity in consideration of inflow, total flood volume, and duration.

The methodology presented in previous studies was applied (Ouyang and Duenas-Osoria, 2012; Song et al., 2019), which quantified performance changes for flooding events in the UDS over time. The analytical framework consists of the following factors: 1) Absorption (Ab), the ability of drainage infrastructure to absorb a defined amount of rainwater to maintain its original condition and prevent runoff to the urban surface; 2) Recovery (Re), the ability of drainage infrastructure to return to a new equilibrium state after rainwater-induced runoff from the urban surface; and 3) changes in sum of the time taken to absorption and recovery after the implementation of green-gray infrastructure strategies. This method is highly relevant because it uses objective results as evaluation criteria, which are easily obtainable from rainfall-runoff models.

The conceptual framework can be understood from Fig. 5 and assumes the following characteristics: the performance of the existing drainage infrastructure is maintained in a steady-state equilibrium; heavy rains cause damage to drainage infrastructure; the performance of the drainage infrastructure passes through a transient state after a disturbance at a certain point in time. After a gradual decrease in performance, a new steady-state equilibrium is reached. In general, following improvements, the absorption phase becomes longer (Ab' > Ab), and the recovery phase becomes shorter (Re' < Re).

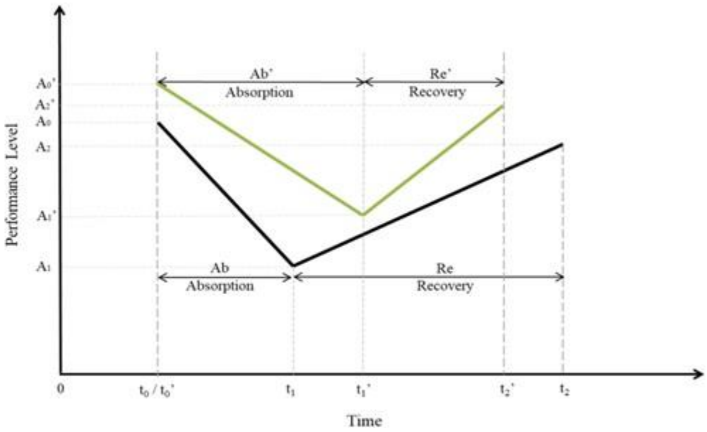

Fig. 12. Conceptual framework for time-dependent UDS performance analysis (Song et al., 2019)

3.3. Results and Discussion

3.3.1 Calibration of the model

The rainfall data of flooding events from 2010–2013 were used to calibrate the simulation. The data were applied to set the parameters of the SWMM using several calibration cycles. After the calibration process, all parameter values of the coupling model were obtained.

Table 6. Precipitation data used for calibration

Rainfall events	Duration time	Sum of precipitation	Maximum hourly precipitation
2010.09.21. 08:00 - 22:00	14-hr	292.5 mm	71.0 mm
2011.07.27. 15:40- 2011.07.28. 22:40	30-hr	414.5 mm	58.0 mm
2013.07.22. 5:40-9:20	3.7-hr	140.0 mm	58.0 mm

The updated simulation results obtained from repeatedly executing the variable adjustments corresponded with the points (nodes 02, 04, 06, 12, 13, and 15 in 2010; nodes 02, 04, 06, 12, 13, and 15 in 2011; nodes 06, 07, and 09 in 2013) where overflow occurred on the flood inundation map. The flood inundation map that was used in this study only contained spatial data; therefore, any comparison with volume-based simulation results was limited. However, assuming that the flood depth was approximately constant and that the elevations of flood inundation locations were similar, the updated simulation results showed a high correlation (R^2) with observational data (Fig. 13).

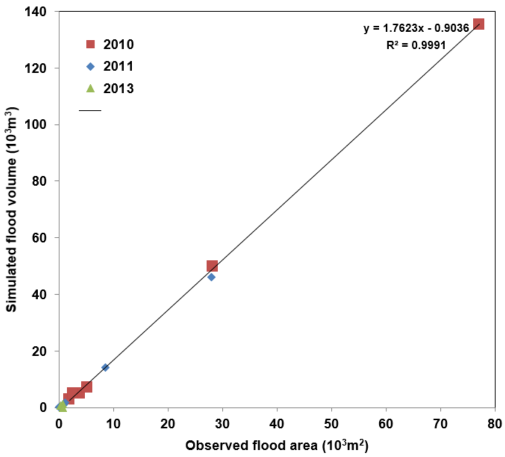

Fig. 13. Correlation between observed flood area and simulated flood volume for nodes in 2010, 2011 and 2013

The SWMM was calibrated by changing Manning's roughness coefficient, infiltration rates, and depression storage for permeable and impermeable spaces in all sub-catchments. Observational data on flood events occurring in the region from 2010, 2011, and 2013 were used for the correction and verification process, and the observed flooding traces and simulated flow rates were compared.

Table 7. Simulation parameters applied to SWMM model

Parameter	Description	Value [Units]
Max. infiltration rate	Maximum rate on the Horton infiltration curve	3.0 [mm/h]
Min. infiltration rate	Minimum rate on the Horton infiltration curve	0.5 [mm/h]
Decay constant	Decay constant for the Horton infiltration curve	4.0 [1/h]
N-Imperv	Manning's n for impervious fraction of sub-catchment	0.016 [$s/m^{1/3}$]
N-Perv	Manning's n for pervious fraction of sub-catchment	0.239 [$s/m^{1/3}$]
Dstore-Imperv	Depth of depression storage of the impervious fraction	6.350 [mm]
Dstore-Perv	Depth of depression storage of the pervious fraction	12.7 [mm]

3.3.2 Effectiveness of green infrastructure implementation

The hydrological response of the catchment differed according to storm characteristics in the baseline scenario (S1). Under the same rainfall intensity conditions, both runoff and flood peak flows were higher in the short-term and 2nd-quartile rainfall conditions than in the long-term and 3rd-quartile rainfall conditions. The hydrological performance of GI scenarios, including GRs and PPs, for 20 rainfall events was investigated and the results are shown in Fig. 14. The decrease and delay of the runoff and flood peak flows for various types of rainfall events can be noted. These results correspond to the properties of each GI practice, and it is considered that this is due to the different installation areas within the target study area (GRs: 27.5 ha; PPs: 5.9 ha). When both GI practices were implemented, it was observed that the peak runoff decreased by 12.9 and 15.6% for the 5-year and 10-year return periods, respectively. However, as the rainfall intensity increased, the peak flow rate reduction effect of GI showed a decreasing trend, which is consistent with the results of various previous studies (Fletcher et al., 2015; Zevenbergen et al., 2018; Mei et al., 2018). In particular, the trend was more pronounced in 6-hour continuous rainfall events than in 3-hour continuous rainfall events. Similarly, the trend was more pronounced for 3rd-quartile rainfall events than 2nd-quartile rainfall events. In case of a 6-hour continuous rainfall event for the 2nd-quartile, it was confirmed that the GI implementation effects were negligible from the 50-year return period, while they were almost non-existent from the 30-year return period for the 3rd-quartile. A similar pattern to the runoff control effects was observed for flood volumes under various rainfall patterns. When both GI practices were installed, the flood mitigation effect was 100% in low-intensity rainfall (5-year return period), and the average flood reduction rate was 38.2%.

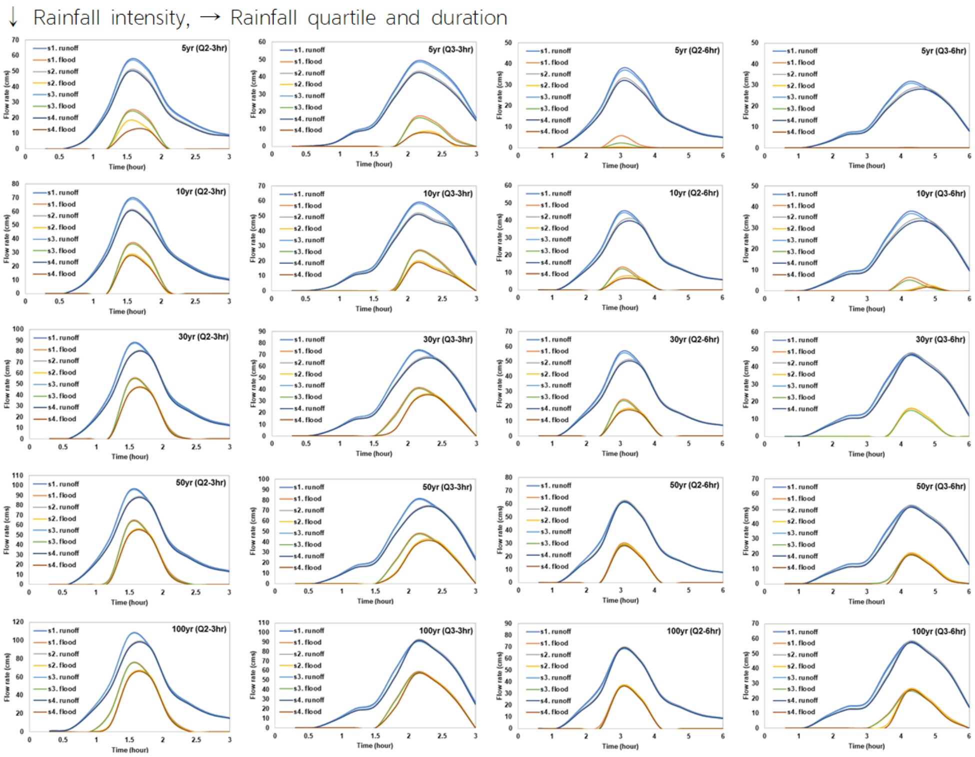

Fig. 14. Hydrographs of the GI scenarios (S1~S4) under 20 rainfall events

To summarize the effects of the rainfall pattern, peak flow rate and V_r are presented in Fig. 15. PPs were not significantly affected by rainfall patterns, and GRs had a greater runoff volume reduction effect in rainfall events with a short duration. The different time distributions (quartiles) did not have a significant impact to runoff volume, but the reduction rate for peak flow rate was generally higher in 2nd-quartile rainfall than in the 3rd-quartile. In particular, the rate of reduction in peak flow rate sharply fell from the 30-year return period rainfall, reaching an ineffective level.

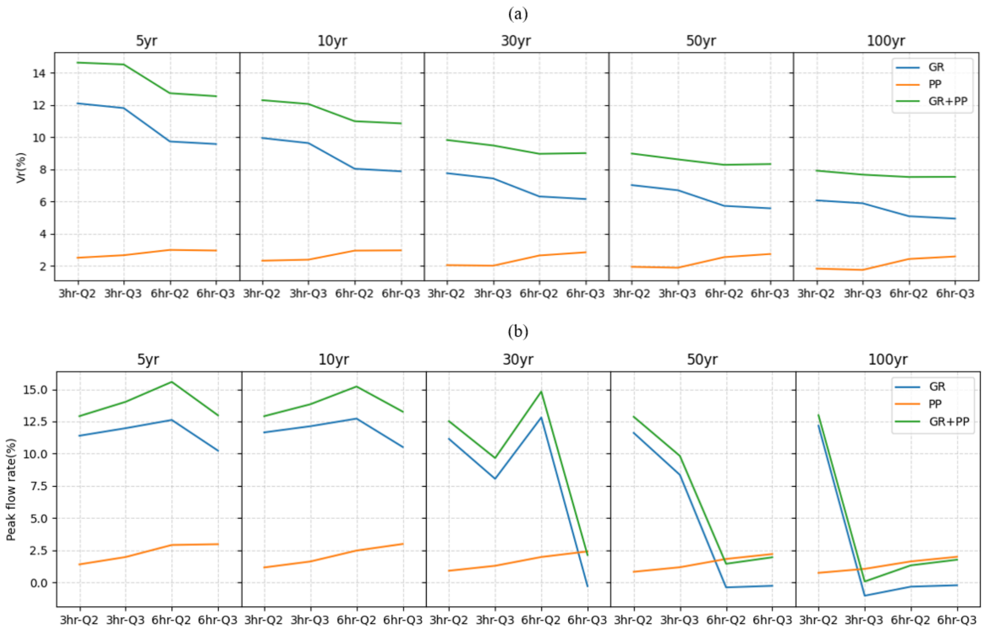

Fig. 15. Reduction rates of (a) peak flow rate and (b) runoff volume in the system for green infrastructure scenarios

3.3.3 Effectiveness of green-gray infrastructure implementation

Our aim was to improve UDS as a gray infrastructure in this section, which included expanding existing or establishing new pipelines. Data on improvements to the UDS are presented in Fig. 11. In addition, the scenarios representing the conditions before and after the improvements in the UDS for 20 rainfall events and the implementation of GI to the improved UDS were compared (Fig. 16). Contrary to the results showing the effects of GI implementation, improvements to the UDS had a negligible effect on the peak flow rate of runoff; however, it affected the peak flow rate of floods.

Following improvements to the UDS, low-intensity rainfall (5-year, 10-year return periods) showed a 100% flood mitigation effect, with an average flood reduction rate of 43.2%. When UDS improvements and GI practices were combined, the average flood reduction rate was 62.2%.

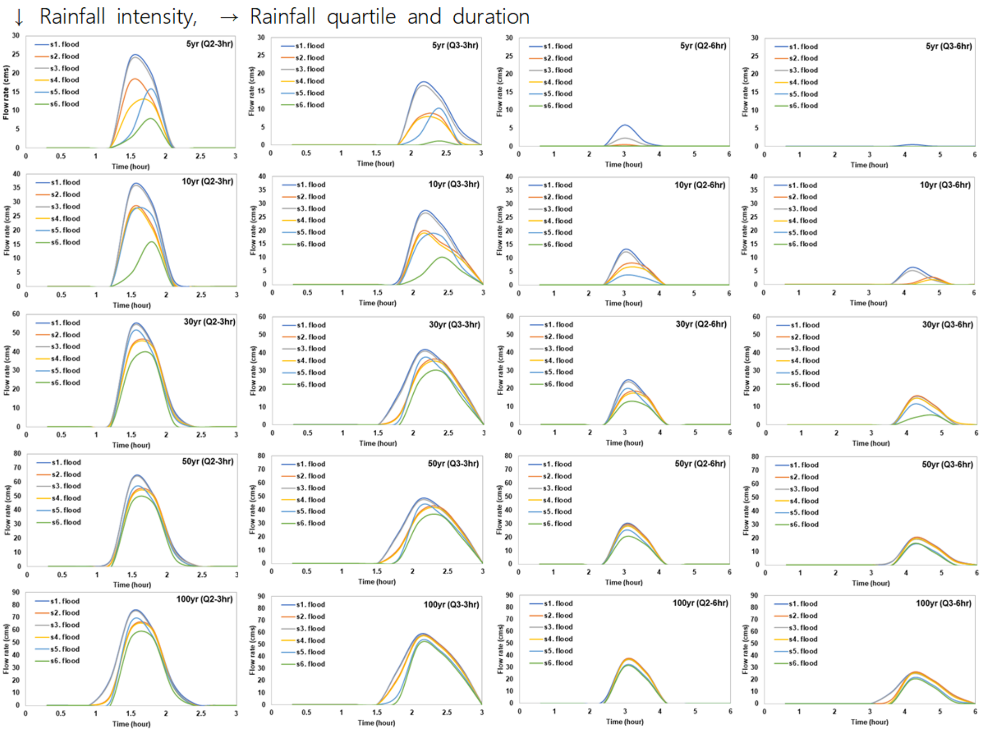

Fig. 16. Flood hydrographs of the green-gray combination scenarios (S1~S6) under 20 rainfall events

To summarize the effects of the rainfall pattern, V_f is presented in Fig. 17. In terms of the flood volume reduction effect, it was confirmed that UDS2 and GR+PP had similar effects in 5-year return period rainfall, and from 10-

year return period rainfall, the effect of UDS2 gradually exceeded the effect of GR+PP. Unlike the characteristics of runoff, the reduction rate for flood volumes was higher in long-term rainfall than in short-term rainfall. The time distribution differences generally did not have a significant effect on flood volumes, but in long-term rainfall, the effect was higher in 3rd-quartile rainfall than in the 2nd-quartile. The reason why storm characteristics have different effects depends on runoff and flood volume is probably due to soil saturation and low-peak intensity storm effects in long duration of rainfall.

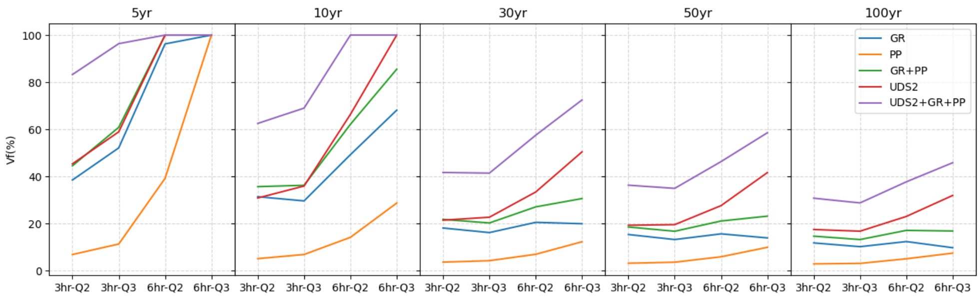

Fig. 17. Reduction rates of flood volume in the system for green-gray infrastructure scenarios

3.3.4 Flood resilience

Time-dependent resilience assessment for S1 and S6 was conducted for two real flood events (10-year return period). As a result of examining the changes in the resilience by the entire system and detailed location as shown in Table 8, there was no time-dependent effect in both events and only the volume reduction effect at the entire system (Fig. 18). However, when looking at the results for each detailed sub-area, there was a time reduction effect in some nodes, and the recovery time decreased in node 6 in 2010. This seems to be due to the fact that there was new construction of pipeline in the UDS2 scenario.

Table 8. Resilience changes by flood events

Flood event	factor	Ab'-Ab	Re'-Re	Time-saving effect on flooding
2010. 09.21	system	0	0	0
	node 4	60min	-60min	0
	node 6	0	-120min	120min
	node 13	65min	-65min	0
	node 2,9,11	flood → no flood		
2011 07.27-28	system	0	0	0
	node 4	0	0	0
	node 11	0	0	0
	node 13	0	0	0
	node 6,9	flood → no flood		

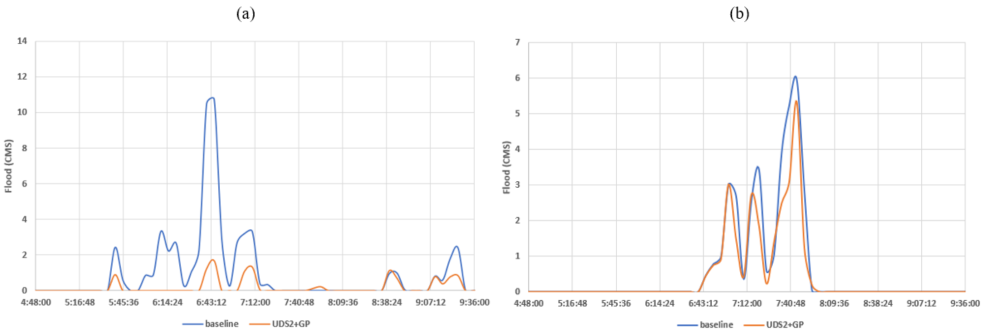

Fig. 18. Changes in flood flow rate at the entire system between S1 and S6

3.4. Conclusions

The main conclusions are summarized as follows: 1) Simulated results confirmed the effects of implementing GI practices on urban flood mitigation in the target study area; 2) among GI practices, the performance of GRs was better than that of PPs; 3) it was confirmed that the peak runoff reduction effect of GI decreased as the return period of the design storm increased, and the effect was almost eliminated at intensities above the 30-year to 50-year return periods; 4) the implementation of GI practices eliminated flooding events for 5-year return period, 6-hour duration, and 3rd-quartile rainfall events; 5) the results showed that the implementation of GI practices should be combined with the improvement of gray infrastructure to achieve optimal flood mitigation under extreme rainfall events.

In the scenario where green and gray infrastructure practices were combined, flooding was eliminated. This included a 10-year return period, 6-hour duration, and 3rd-quartile rainfall event. Different results were obtained depending on hydrological performance index used; the gray infrastructure affected flood reduction but not the peak flow of runoff. In addition, the longer the rainfall duration, the lower the runoff volume reduction effect of green-gray infrastructure. However, the flood reduction effect showed the opposite result. When the average flood reduction rates for all rainfall events were calculated, it was found that the implementation of GI reduced flooding by 38.2%, improvement of gray infrastructure reduced flooding by 43.2%, and both options when jointly implemented reduced flooding by 62.2%.

There were several limitations to this study. First, the area used for the possible implementation of PPs was limited, and it was therefore challenging to accurately compare the performance of GRs. The second limitation is also similar to the first, since the gray infrastructure installation condition used in this study is a change applied to the real city, there was a limit to comparing the exact difference in effect with the green infrastructure.

This work demonstrates that the proposed evaluation technique can contribute to assessing the performance of green-gray infrastructure projects. The results highlight the importance and necessity of detailed comparisons of various options that can aid the decision-making process governing green-gray infrastructure planning. In this study, performances were assessed for various scenarios. However, performance should also be compared while considering the costs of investment in order to select a reasonable strategy.

IV. Optimized placement of green-gray infrastructure for effective flood mitigation

4.1. Introduction

Urban flooding negatively impacts infrastructure and humans and can lead to excessive damage costs (IPCC, 2014). Therefore, urban flood management (UFM) is essential for effectively managing the physical causes and potential effects of flooding by improving the structure and function of cities (Merz et al., 2010). Although there is a large body of literature on flood mitigation and management strategies, such as structural flood protection, sustainable urban drainage systems (SUDS), and GIs (Ghofrani et al., 2017; Dawson et al., 2020), relatively few studies have documented spatial impacts that can inform urban planners and flood management practitioners to manage excessive runoff in urban systems (Nguyen et al., 2019). In relation to the study of spatial effects, it was initially assumed that flooding occurred downstream, mainly due to the upstream flow (Horton, 1945). Later, the term variable source area (VSA) was discussed, highlighting that land use contribution to the drainage catchment differs in space and time (Woldesenbet et al., 2017; Yan et al., 2016). The VSA is a concept in which most runoff catchment is driven by a relatively small fraction of the runoff sources, which can increase or decrease with time and spatial variability (Hibbert and Troendle, 1988).

Subsequent studies on VSA have improved the understanding of the flooding process by identifying the importance of several parameters influencing floodings, such as land cover, topography, and soil characteristics (Miles and Band, 2015).

Various research methods, such as stochastic, empirical, probabilistic and deterministic methods, have been used to analyze the impact of urban flooding (Escuder-Bueno et al., 2012). Among them, deterministic methods using a hydrological model based on a simplified representation of the 'real world' are appropriate for identifying hazardous areas or confirming the effectiveness of spatial techniques such as green-gray infrastructures (Rodriguez et al., 2021). Hydrologic and hydraulic modeling has been used to answer VSA questions regarding flood risk management (FRM) (Jajarmizadeh, 2012; Teng et al., 2017). These include studies that identify hazardous areas or evaluate the contribution of each domain to system runoff (Teng et al., 2017; Dawson et al., 2020).

It is important to demonstrate strategies that can be implemented to reduce the flow at flooding sources and minimize flood risk at critical locations (Vleeschauwer et al., 2014; Fletcher et al., 2015; Dawson et al., 2020). Although GI is a suitable control measure to reduce runoff, modeling guidelines for its effective implementation are lacking (Saghafian and

Khosroshahi, 2005; Petrucci et al., 2013; Saghafian et al., 2015). Therefore, this study conducted a modeling research based on an actual target site to confirm the hypothesis that it is appropriate to install GI in the source area and to take structural protection measures in the impact area, as summarized in previous studies. The research method suggested by Dawson et al. (2020) was applied to derive the source and impact areas, and the spatial impact was analyzed by applying the green-grey infrastructure application technique for each area.

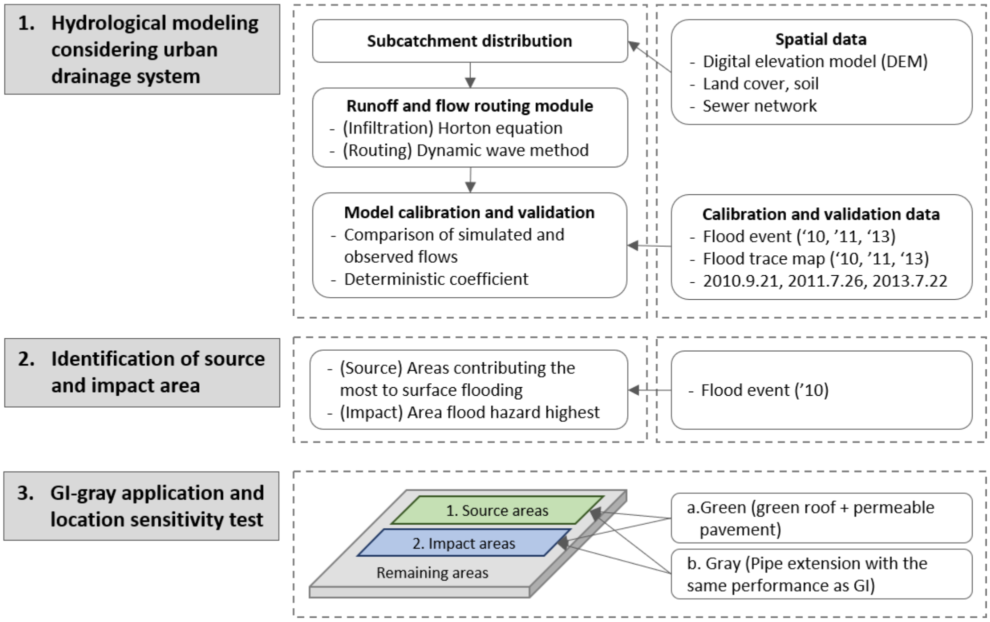

Fig. 19. Research framework of the study

4.2. Methods

4.2.1 Case study

The case study site is located in Seoul, the capital of South Korea, which is one of the most densely populated cities worldwide. The case site was selected at the catchment scale, which represents the basic scale for determining the amount of domestic water in urban areas and minimizing other impacts. This site is a typical commercial area with an area of 192.61 ha, an elevation of 14–71 m, and an impermeable area of 85%. In addition, the site has a history of flooding (1984, 1990, 1998, 2001, 2010, 2011, and 2013), despite sewer construction.

Precipitation data in 2010 collected at the automated weather station (AWS) of Gangnam (37.5131° N, 127.0470° E), which was the nearest rain gauge to the site, was measured at a resolution of 5 min. The maximum 2-hour rainfall for flood event in 2010 was 128.5mm, which is equivalent to 25-year return period rainfall (Fig. 20). According to national statistics, property damage in Seoul, including the loss of roads and flooding of houses in 2010, was estimated to be 14.5 million USD (KMA, 2010).

Table 9. Precipitation data of flood inundation event

Rainfall events	**Duration time**	**Sum of precipitation**	**Maximum hourly precipitation**
2010.09.21. 08:00 - 22:00	14-hr	292.5 mm	71.0 mm

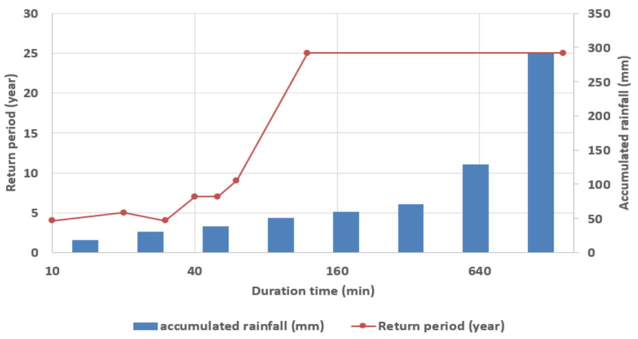

Fig. 20. Return period by duration time of 2010 flood event

4.2.2 Source and impact area

Areas requiring green-gray infrastructure were selected by considering two main aspects; a set of flooded area (impact) and the most flood-contributing area (source). This process is a source-impact-based priority area identification methodology proposed by Vercruysse et al. (2019) and was performed using the ArcGIS Desktop v10.5. The following simulation-based analysis is performed to explore areas with the highest flood contribution: (1) modeling to analyze the flooding volume for a specific rainfall event in the entire study area, (2) executing a model repeatedly that omits rainfall in individual sub-catchments, (3) defining the difference between values (1) and (2) as the flood contribution of individual sub-catchment. While Vercruysse et al. (2019) used a grid-based model, there are some differences in the methodology that this study used a semi-distributed model to include the impact of the urban drainage system.

4.2.3 Hydrological model

All hydrodynamic analyses in the study were performed using a sewer network model implemented in SWMM version 5.1, which is one of the few models available with the capability to simulate the hydrological responses of GI practices (Rossman, 2010). Model composed by Bae et al. (2020) was used, which includes 16 sub-catchments that drain into 16 junction nodes connected to 15 conduit links. Infiltration refers to the process by which rainfall is absorbed into the underground surface and penetrates the unsaturated soil area, and Horton's method is applied in the model. Flow routing was simulated using the dynamic wave method.

The model was calibrated by changing the Manning's coefficient, infiltration rates and depression storage for both permeable and impermeable fractions of all the sub-catchments. For the calibration processes, rainfall data of 5-minute temporal resolution between 2010 and 2011 were used. Calibration process were based on comparison of the simulated flood volume for each node and observed flood trace. The deterministic coefficient R^2 is used to assess the degree of correlation between the simulated and observed output (Chapter 3.3.1).

4.2.4 Green-gray infrastructure scenarios

GI techniques were implemented by integrating green roofs (GR) and permeable pavements (PP), suitable for installation in existing infrastructures. In SWMM, the GI technique was expressed using a combination of vertical layers of surface, soil, and storage, and the design elements for each layer were applied using the parameters suggested in previous studies (Rodriguez et al., 2021; Abualfaraj et al., 2018; Tirpak et al., 2021; Randall et al., 2019).

Table 10. Summary of GI characteristics

	Parameter	**Permeable pavement**	**Green roof**
Surface	Bern height [mm]	5	75
	Vegetation volume fraction	0	0.1
	Roughness (Mannings n)	0.05	0.1
	Slope	2	0.3
Soil/Sand	Thickness [mm]	-	150
	Porosity	-	0.4
	Field capacity	-	0.105
	Wilting point	-	0.047
	Conductivity [mm/hr]	-	72
	Suction head [mm]	-	20
Pavement	Thickness	150	-
	Void ratio	0.4	-
	Impervious surface fraction	0.3	-
	Permeability [mm/h]	72	-
Storage / Drainage mat	Thickness [mm]	150	50
	Void fraction	0.5	0.55
	Seepage rate [mm/hr]	78	-
	Roughness (Mannings n)	-	0.3

In this study, other conditions, such as the application area, were set equally to compare the performance considering only the ‘application location’ of the green-gray infrastructure. GI of the same area was allocated to the source and impact areas. However, it was adjusted to not exceed the maximum allowable area by reflecting the land cover characteristics in the research area. In addition, we matched characteristics of green and gray infrastructures using the methods in Chapter 2.3.2 and Fig. 4, which were derived from the results of sensitivity test on expansion rate of conduit cross-section area with the same hydrological performance as the green infrastructure. This is based on a test on how much flood reduction effect similar to how much pipe expansion is performed in the entire catchment when green infrastructure is installed in the entire catchment, and as a result, a value of 13% was derived. The cross-sectional height of the conduit required to expand the cross-sectional area of the conduit by 13% was presented for each sub-catchment, and the application area of the green infrastructure was also presented (Table 11). This process was conducted because the same conditions must be set for a clear comparison between green and gray infrastructure, and in this study, the same conditions were set based on 'hydrological performance'.

Table 11. Summary of green-gray infrastructure implementation

Spatial division	Sub-catchment number	Application condition			
		Gray (conduit cross-sectional height)			Green (GR+PP)
		Original (m)	Conduit type	Enlarged (m)	Area (ha)
Source area	3	3.0	closed rectangular	3.4	2.0
	12	3.0	closed rectangular	3.4	2.0
	7	1.2	circular	1.4	4.0
Source-Impact intersection	14	1.2	circular	1.3	4.0
Impact area	2	1.3	circular	1.5	4.0
	16	1.2	circular	1.4	4.0

The scenarios based on green-gray infrastructure changes were divided into 5 cases, including the baseline without any implementation (Table 12). First of all, as mentioned in the research purpose, we tried to compare S1 and S2 to confirm the hypothesis that it is appropriate to install green infrastructure in the source area and take structural protection measures in the impact area. In addition, the case of adopting only green or gray infrastructure such as S3 and S4, was compared together to analyze the difference in effect.

Table 12. Overview of scenarios modeled in this study

Scenarios	Green infra		Gray infra	
	Source	**Impact**	**Source**	**Impact**
Baseline (no green-gray)	x	x	x	x
S1. Green in source + Gray in impact	○	x	x	○
S2. Green in impact + Gray in source	x	○	○	x
S3. Green in impact and source	○	○	x	x
S4. Gray in impact and source	x	x	○	○

4.3. Results and discussion

4.3.1 Source and impact area identification

Values assigned to individual sub-catchment for “impact” and “source” are classified into three classes based on the Natural Breaks technique. The highest-class area is set as the green-gray infrastructure placement area. A description of the methodology and the result of area derivation for green-gray infrastructure placement is presented in Fig. 21.

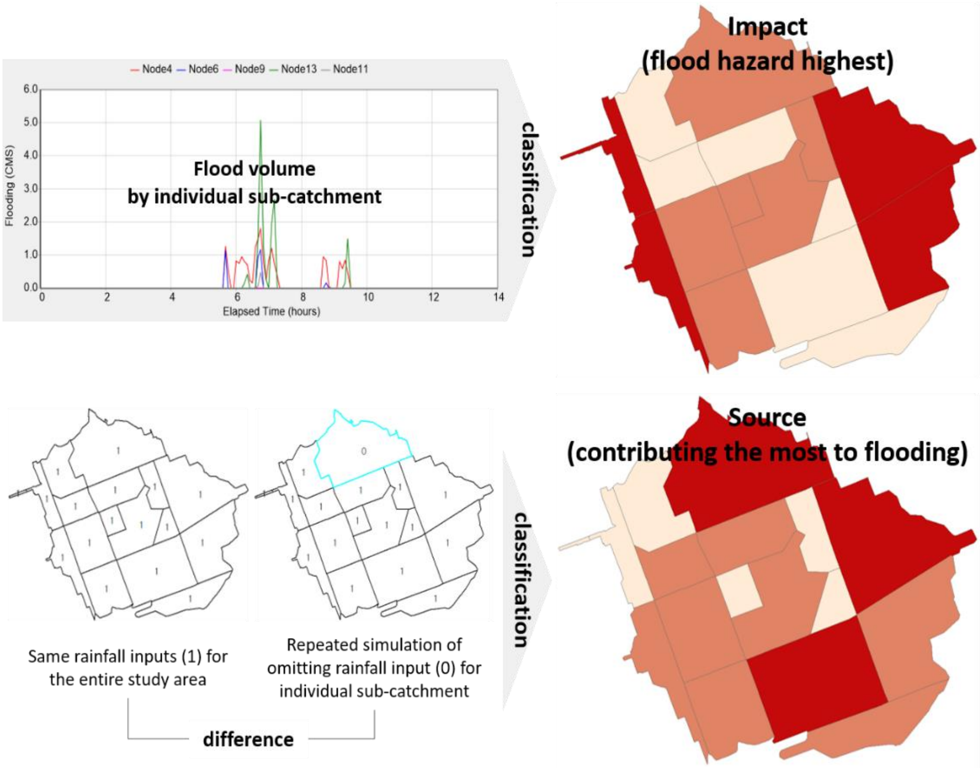

Fig. 21. Source and impact area derivation for green-gray infrastructure placement

4.3.2 Comparison of effect difference

As in the research hypothesis, installing green infrastructure in the source area and gray infrastructure in the impact area showed the greatest effect in reducing flooding. When only green infrastructure was applied to both areas (S3), the flood reduction effect was somewhat lower than that of the best case (S1). The advantage of S3 in runoff control seems to be due to its relatively high infiltration capacity. Table 13 presented the results for each scenario of main output performance index such as runoff depth, flood volume, infiltration depth and peak runoff flow rate.

Table 13. Overview of results by scenarios

	Runoff (mm)	**Flood (1,000m^3)**	**Infiltration (mm)**	**Peak runoff (CMS)**
Baseline (no green-gray)	264.0	16.7	0.7	33.7
S1. Green in source + Gray in impact	255.0	3.9	3.2	31.4
S2. Green in impact + Gray in source	257.9	12.6	4.4	31.5
S3. Green in impact and source	248.7	5.6	7.0	31.4
S4. Gray in impact and source	264.0	9.3	0.7	33.8

As a result of summarizing the flood hydrograph for S1~S2 and baseline (Fig. 22), it was confirmed that the flood was removed from both S1 and S2 compared to the baseline. When S1 and S2 were compared, no peak flood delay effect was found, but the flooding start time was delayed by 60 minutes. In addition, in sub-catchment 3, where hazard was the highest, the flood amount of S1 was reduced by 30.4% and S2 by 88.9% compared to baseline, showing a large difference in effect.

The reduction rate for flood volume and runoff depth was derived compared to the baseline for S1~S4 in Fig. 23. It is noteworthy here that the reduction effect of the flood volume was the best in S1, but the reduction effect for the runoff depth was the best in S3, which applied only the green infrastructure. The cause of these results seems to be that the source-impact area in the research method was based on the amount of flooding. Therefore, it suggests that the target management area may also change depending on whether the reduction goal is in “surface runoff” or “flood”.

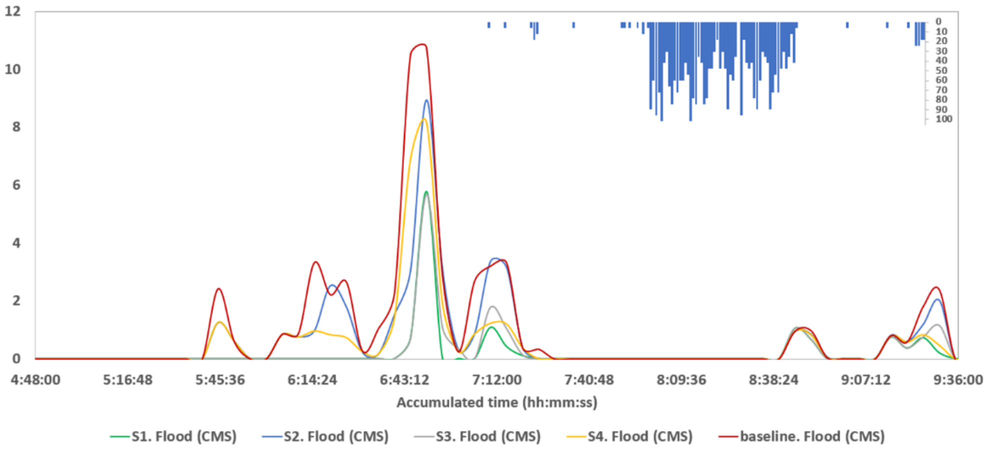

Fig. 22.Flood hydrograph in 2010 flood event for S1~S4 and baseline

The green infrastructure scenario presented in this study was established based on the assumption that the entire building and sidewalk exist in the target site. However, considering that the green roof created for about 20 years ('02~'20) in Seoul, which is about 300 times the area of the target site, is about 1ha (Seoul city, 2021), the scenario set in this study (12 ha of green infrastructure) is not realistic. Nevertheless, research on the maximum effect is important in setting policy goals, as green roofs and street greening are increasing the installation goal every year (1 ha in 2021) due to the advantage of easy installation in highly-developed urban areas.

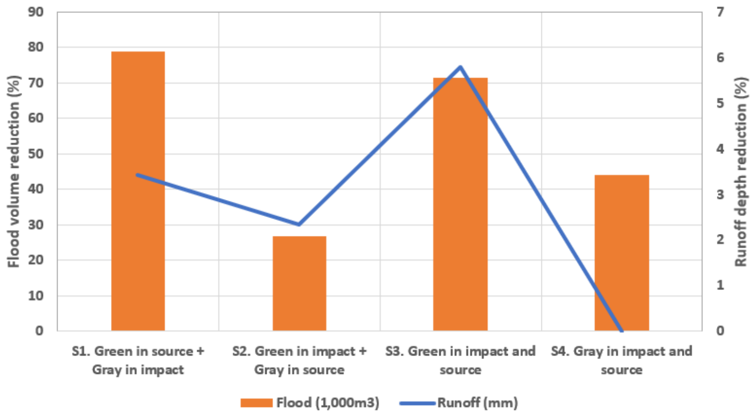

Fig. 23. Flood and runoff reduction rate by scenarios

4.4. Conclusion

This study used a hydrologic model based on the source-impact area classification guide in catchments to evaluate the spatial effects of flooding and explore the effectiveness of green-gray infrastructure on the urban catchment scale. It was confirmed that implementing GI in areas that induce flooding and gray infrastructure in areas impacted by floods are advantageous for flood reduction. However, the performance index related to runoff found that the scenario of installing only green infrastructure was more advantageous. This is thought to be because the source-impact area set in this study is derived based on the flood volume, and this result means that policy implications may vary depending on which hydrological performance index is targeted.

The result of this study is not general for all rainfall events and can be affected by various rainfall intensities and durations. Therefore, further research should investigate the effects of rainfall intensity and the timing of events. In addition, since the sub-catchment area is roughly divided, the spatial resolution of the results was low, making it difficult to consider the implications for the detailed area, so it is necessary to increase the spatial resolution of the model to improve accuracy. Furthermore, this study tried to set the conditions of the green-gray infrastructure equally based on “hydrological performance”, matching conditions based on “cost” to present policy implications can be an alternative.

This study will contribute to demonstrating the effectiveness of strategies that can be implemented to reduce the flow at flooding sources and minimize the risk of flooding in critical locations in terms of spatial planning and regeneration

V. Conclusions

This study aimed to provide information for green-gray infrastructure planning, which is desirable when considering the interaction between existing and new infrastructure regarding urban flood management. With increased complex city structures and variability of rainfall patterns, it is important to analyze the spatiotemporal impact during green-grey infrastructure planning. SWMM, a distributed hydrologic model, was used to analyze the effectiveness of various spatiotemporal green-gray infrastructure implementation scenarios, and the accuracy of the simulation results was improved through model updates based on sensitivity tests and parameter estimations according to actual rainfall events.

A flood reduction effect was derived from the GI technique; however, a better flood reduction effect was derived from the green-grey combination technique. GI effects gradually decreased as rainfall intensity surpassed a 30-year return period. However, given that flooding in cities is generally a 10-year return period, GI will likely withstand many cases of rainfall. Under various rainfall patterns, there are varying characteristics in the reduction effect between flooding and runoff; therefore, green-gray infrastructure planning goals may vary depending on which indices are considered.

This study had other limitations. First, it is important to ensure model accuracy to present consistent implications under various conditions, which requires using improved observation data in the calibration process and the optimization of many parameters. Second, this study describes the results based on discussions of hydrological performance; however, to provide information on decision-making, implications linked to costs are required.

This study demonstrates that the proposed evaluation technique can help evaluate the performance of green-grey infrastructure. The results highlight the importance and necessity of detailed comparisons of various options in the decision-making process of green-gray infrastructure planning.

VI. Bibliography

Dawson, D.A., Vercruysse, K., Wright, N., 2020. A spatial framework to explore needs and opportunities for interoperable urban flood management. Philos. Trans. R. Soc. A Math. Phys. Eng. Sci. 378. https://doi.org/10.1098/rsta.2019.0205

Dushkova, D., Haase, D., 2020. Not simply green: Nature-based solutions as a concept and practical approach for sustainability studies and planning agendas in cities. Land 9. https://doi.org/10.3390/land9010019

Ercolani, G., Chiaradia, E.A., Gandolfi, C., Castelli, F., Masseroni, D., 2018. Evaluating performances of green roofs for stormwater runoff mitigation in a high flood risk urban catchment. J. Hydrol. 566, 830–845. https://doi.org/10.1016/j.jhydrol.2018.09.050

Fletcher, T.D., Shuster, W., Hunt, W.F., Ashley, R., Butler, D., Arthur, S., Trowsdale, S., Barraud, S., Semadeni-Davies, A., Bertrand-Krajewski, J.L., Mikkelsen, P.S., Rivard, G., Uhl, M., Dagenais, D., Viklander, M., 2015. SUDS, LID, BMPs, WSUD and more – The evolution and application of terminology surrounding urban drainage. Urban Water J. 12, 525–542. https://doi.org/10.1080/1573062X.2014.916314

Huang, Y., Tian, Z., Ke, Q., Liu, J., Irannezhad, M., Fan, D., Hou, M., Sun, L., 2020. Nature-based solutions for urban pluvial flood risk management. WIREs Water 7, 1–17. https://doi.org/10.1002/wat2.1421

Kuller, M., Bach, P.M., Ramirez-Lovering, D., Deletic, A., 2017. Framing water sensitive urban design as part of the urban form: A critical review of tools for best planning practice. Environ. Model. Softw. 96, 265–282. https://doi.org/10.1016/j.envsoft.2017.07.003

Maes, J., Barbosa, A., Baranzelli, C., Zulian, G., Batista e Silva, F., Vandecasteele, I., Hiederer, R., Liquete, C., Paracchini, M.L., Mubareka, S., Jacobs-Crisioni, C., Castillo, C.P., Lavalle, C., 2015. More green infrastructure is required to maintain ecosystem services under current trends in land-use change in Europe. Landsc. Ecol. 30, 517–534. https://doi.org/10.1007/s10980-014-0083-2

Merz, B., Kreibich, H., Schwarze, R., Thieken, A., 2010. Review article “assessment of economic flood damage.” Nat. Hazards Earth Syst. Sci. 10, 1697–1724. https://doi.org/10.5194/nhess-10-1697-2010

Nesshöver, C., Assmuth, T., Irvine, K.N., Rusch, G.M., Waylen, K.A., Delbaere, B., Haase, D., Jones-Walters, L., Keune, H., Kovacs, E., Krauze, K., Külvik, M., Rey, F., van Dijk, J., Vistad, O.I., Wilkinson, M.E., Wittmer, H., 2017. The science, policy and practice of nature-based solutions: An interdisciplinary perspective. Sci. Total Environ. 579, 1215–1227. https://doi.org/10.1016/j.scitotenv.2016.11.106

Nguyen, H.Q., Radhakrishnan, M., Bui, T.K.N., Tran, D.D., Ho, L.P., Tong, V.T., Huynh, L.T.P., Chau, N.X.Q., Ngo, T.T.T., Pathirana, A., Ho, H.L., 2019. Evaluation of retrofitting responses to urban flood risk in Ho Chi Minh City using the Motivation and Ability (MOTA) framework. Sustain. Cities Soc. 47, 101465. https://doi.org/10.1016/j.scs.2019.101465

O'Donnell, T., 2019. Contrasting land use policies for climate change adaptation: A case study of political and geo-legal realities for Australian coastal locations. Land use policy 88, 104145. https://doi.org/10.1016/j.landusepol.2019.104145

Qin, Y., He, Y., Hiller, J.E., Mei, G., 2018. A new water-retaining paver block for reducing runoff and cooling pavement. J. Clean. Prod. 199, 948–956. https://doi.org/10.1016/j.jclepro.2018.07.250

Ruangpan, L., Vojinovic, Z., Di Sabatino, S., Leo, L.S., Capobianco, V., Oen, A.M.P., Mcclain, M.E., Lopez-Gunn, E., 2020. Nature-based solutions for hydro-meteorological risk reduction: a state-of-the-art review of the research area. Nat. Hazards Earth Syst. Sci. 20, 243–270. https://doi.org/10.5194/nhess-20-243-2020

Salinas-Rodríguez, S.A., Sánchez-Navarro, R., Barrios-Ordóñez, J.E., 2021. Frequency of occurrence of flow regime components: a hydrology-based approach for environmental flow assessments and water allocation for the environment. Hydrol. Sci. J. 66, 193–213. https://doi.org/10.1080/02626667.2020.1849705

Vercruysse, K., Dawson, D.A., Glenis, V., Bertsch, R., Wright, N., Kilsby, C., 2019. Developing spatial prioritization criteria for integrated urban flood management based on a source-to-impact flood analysis. J. Hydrol. 578, 124038. https://doi.org/10.1016/j.jhydrol.2019.124038

Intergovernmental Panel on Climate Change (IPCC), 2014. Climate Change 2014: Synthesis Report; Contribution of Working Groups I, II and III to the Fifth Assessment Report of the Intergovernmental Panel on Climate Change; Pachauri, R.K. Meyer, L.A., Eds.; IPCC: Geneva, Switzerland.

Yoon, S., Moon, Y, 2009. Urban flood damage mitigation and countermeasure method establishment: Focused on Seoul city, J. Korea Water Resour. Associ., 42, 59-65. (In Korean)

Intergovernmental Panel on Climate Change (IPCC), 2012. Managing the Risks of Extreme Events and Disasters to Advance Climate Change Adaptation; A

Special Report of Working Groups I and II of the Intergovernmental Panel on Climate Change; Field, C.B., Barros, V., Stocker, T.F., Qin, D., Dokken, D.J., Ebi, K.L., Mastrandrea, M.D., Mach, K.J., Plattner, G.K., Allen, S.K., Tignor, M., Midgley, P.M., Eds.; Cambridge University Press, Cambridge, UK, and New York, USA.

Korea Meteorological Administration, 2017. 2016 abnormal Climate Report; Korea Meteorological Administration, Seoul, Korea. (In Korean)

Graham, P., Kim, M., 2003. Evaluating the stormwater management benefits of green roofs through water balance modeling, In Proceedings of the First North American Conference on Greening Rooftops for Sustainable Communities (GRSC 2003), Chicago, IL, USA.

Maryland Department of Environmental Resources Programs and Planning Division, 1999. Low-impact development: An integrated design approach, Maryland, USA.

Inkiläinen, E.N.M., McHale, M.R., Blank, G.B., James, A.L., Nikinmaa, E., 2013. The role of the residential urban forest in regulating throughfall: A case study in Raleigh, Landsc. Urban Plan. 119, 91–103.

Palla, A., Gnecco, I., La Barbera, P., 2017. The impact of domestic rainwater harvesting systems in storm water runoff mitigation at the urban block scale, J. Environ. Manag. 191, 297-305.

Montalto, F.; Behr, C., 2007. Alfredo, K.; Wolf, M.; Walsh, M. Rapid assessment of the cost-effectiveness of low impact development for CSO control, Landsc. Urban Plan. 82, 117-131.

Dietz, M.E., 2007. Low impact development practices: A review of current research and recommendations for future directions, Water Air Soil Pollut. 186, 351-363.

Ellis, J.B., 2012. Sustainable surface water management and green infrastructure in UK urban catchment planning, J. Environ. Plan. Manag. 56, 24–41.

Kim, H.; Lee, D., 2016. Sung, S. Effect of Urban Green Spaces and Flooded Area Type on Flooding Probability, Sustainability 8(2): 134.

Koh, T.; Lee, W., 2012. Necessity of Planning Urban Basins from Experiences of Flood-damage in Seoul, Urban Policy Res. 3, 57-71. (In Korean)

Ministry of Land, Transport and Maritime Affairs (MLTM), Government of the Republic of Korea. 2011. Probability Rainfall Table. Available from "www.k-idf.re.kr"

Korea Meteorological Administration, 2010. 2010 abnormal Climate Report; Korea Meteorological Administration, Seoul, Korea. (In Korean)

Korea Meteorological Administration, 2011. 2011 abnormal Climate Report; Korea Meteorological Administration, Seoul, Korea. (In Korean)

Singh, V.P., Woolhiser, D.A., 2002. Mathematical modeling of watershed hydrology, J. Hydrol. Eng. 7, 270-292.

Rossman, L., 2010. Storm Water Management Model User's Manual Version 5.0, US EPA Office of Research and Development, Washington, DC, USA.

Bhaduri, B.M., Minner, S., Tatalovich, Harbor, J., 2001. Long-term hydrologic impact of urbanization: a tale of two models, J. Water Resour. Plann. Manage. 127, 13–19.

Tsihrintzis, V.A., Hamid, R., 1998. Runoff quality prediction from small urban catchments using SWMM, Hydrol. Processes. 12, 311–329.

Warwick, J.J., Tadepalli, P., 1991. Efficacy of SWMM application, J. Water Resour. Plann. Manage. 117, 352-366.

Huber, W.C., Dickinson, R.E., 1998. Storm Water Management Model, Version 4: User's Manual, Environmental protection Agency, USA.

Dooge, J.C.I., 1973. Linear theory of hydrologic systems, Agricultural Research Service, U.S. Department of Agriculture, Washington, D.C., USA.

Engman, E.T., 1986. Hydrologic research before after AgRISTARS, IEEE Trans. Geoschi. Remote Sens. 24, 5-11.

American Society of Civil Engineers, 1982. Gravity sanitary sewer design and construction, ASCE manual of practice No. 60, New York, USA.

VanWoert, N.D., Rowe, D.B., Andresen, J.A., Rugh, C.L., Fermandez, R.T., Xiao, L., 2005. Green roof stormwater retention: Effects of roof surface, slope, and media depth, J. Environ. Qual. 34, 1036-1044.

Dunnett, N., Kingsbury, N., 2004. Planting Green Roofs and Living Walls, Portland, OR: Timber Press.

Mentens, J., Raes, D., Hermy, M., 2006. Green roofs as a tool for solving the rainwater runoff problem in the urbanized 21st century?, Landsc. Urban Plan. 77, 217-226.

Obermdprfer, E., Lundholm, J., Bass, B., Coffman, R.R., Doshi, H., Dunnett, N., Gaffin, S., Kohler, M., Liu, K.Y., Rowe, B., 2007. Green Roofs as Urban Ecosystems: Ecological Structures, Functions, and Services, Am. Inst. Biol. Sci. 57, 823-833.

Brattebo, B.O., Booth, D.B., 2003. Long-term stormwater quantity and quality performance of permeable pavement systems, Water Res. 37, 4369-4376.

Lee, J., Yeo, W., Shim, J., Kang, T., 2001. Analysis of Stormwater Runoff Reduction Effects by Using Porous Pavement, Korean Soc. Civ. Eng. 21, 645-654. (In Korean)

Shackel, B., Ball, J., Mearing, M., 2003. Using permeable eco-paving to achieve improved water quality for urban pavements, In Proceedings of the 7th International Conference on Concrete Block Paving (PAVE AFRICA 2003), Sun City, South Africa, 12-15 October 2003.

Seo, K., Son, J., Lee, J., 2011. A new look at Changma. Korean Meteorological Society 21(2) 109-121.

Abualfaraj, N., Cataldo, J., Elborolosy, Y., Fagan, D., Woerdeman, S., Carson, T., Montalto, F.A., 2018. Monitoring and modeling the long-term rainfall-runoff response of the Jacob K. Javits center green roof. Water (Switzerland) 10, 1–23. https://doi.org/10.3390/w10111494

Arjenaki, M.O., Sanayei, H.R.Z., Heidarzadeh, H., Mahabadi, N.A., 2021. Modeling and investigating the effect of the LID methods on collection network of urban runoff using the SWMM model (case study: Shahrekord City). Model. Earth Syst. Environ. 7, 1–16. https://doi.org/10.1007/s40808-020-00870-2

Bertilsson, L., Wiklund, K., de Moura Tebaldi, I., Rezende, O.M., Veról, A.P., Miguez, M.G., 2019. Urban flood resilience – A multi-criteria index to integrate flood resilience into urban planning. J. Hydrol. 573, 970–982. https://doi.org/10.1016/j.jhydrol.2018.06.052

Cosens, B.A., 2013. Legitimacy, adaptation, and resilience in ecosystem management. Ecol. Soc. 18. https://doi.org/10.5751/ES-05093-180103

Damodaram, C., Giacomoni, M.H., Prakash Khedun, C., Holmes, H., Ryan, A., Saour, W., Zechman, E.M., 2010. Simulation of combined best management practices and low impact development for sustainable stormwater management. J. Am. Water Resour. Assoc. 46, 907–918. https://doi.org/10.1111/j.1752-1688.2010.00462.x

Davoudi, S., Shaw, K., Haider, L.J., Quinlan, A.E., Peterson, G.D., Wilkinson, C., Fünfgeld, H., McEvoy, D., Porter, L., 2012. Resilience: A Bridging Concept or a Dead End? "Reframing" Resilience: Challenges for Planning Theory and Practice Interacting Traps: Resilience Assessment of a Pasture Management System in Northern Afghanistan Urban Resilience: What Does it Mean in Planning Practice? Resilience as a Useful Concept for Climate Change Adaptation? The Politics of Resilience for Planning: A Cautionary Note. Plan. Theory Pract. 13, 299–333. https://doi.org/10.1080/14649357.2012.677124

Eckart, K., McPhee, Z., Bolisetti, T., 2017. Performance and implementation of low impact development – A review. Sci. Total Environ. 607–608, 413–432. https://doi.org/10.1016/j.scitotenv.2017.06.254

FA Huff, 1967. Time Distribution Rainall in Heavy Storms be used in hydrologic design problems or. Water Resour. Res. 3, 1007–1019.

Folke, C., 2006. Resilience: The emergence of a perspective for social-ecological systems analyses. Glob. Environ. Chang. 16, 253–267. https://doi.org/10.1016/j.gloenvcha.2006.04.002

Jia, H., Yao, H., Tang, Y., Yu, S.L., Field, R., Tafuri, A.N., 2015. LID-BMPs planning for urban runoff control and the case study in China. J. Environ. Manage. 149, 65–76. https://doi.org/10.1016/j.jenvman.2014.10.003

Joshi, P., Leitão, J.P., Maurer, M., Bach, P.M., 2021. Not all SuDS are created equal: Impact of different approaches on combined sewer overflows. Water Res. 191, 116780. https://doi.org/10.1016/j.watres.2020.116780

Leandro, J., Chen, K.F., Wood, R.R., Ludwig, R., 2020. A scalable flood-resilience-index for measuring climate change adaptation: Munich city. Water Res. 173, 115502. https://doi.org/10.1016/j.watres.2020.115502

Lee, S., 2018. Statistical significance test of polynomial regression equation for Huff's quartile method of design rainfall. J. Korea Water Resour. Assoc. 51, 263–272. https://doi.org/10.3741/JKWRA.2018.51.3.263

Li, M.Y., Yang, Y.L., Liu, L., Wang, L., 2016. Effects of social support, hope and resilience on quality of life among Chinese bladder cancer patients: A cross-sectional study. Health Qual. Life Outcomes 14, 1–9. https://doi.org/10.1186/s12955-016-0481-z

Mei, C., Liu, J., Wang, H., Shao, W., Xia, L., Xiang, C., Zhou, J., 2018. Modelling the ability of source control measures to reduce inundation risk in a community-scale urban drainage system. Proc. Int. Assoc. Hydrol. Sci. 379, 223–229. https://doi.org/10.5194/piahs-379-223-2018

Mugume, S.N., Gomez, D.E., Fu, G., Farmani, R., Butler, D., 2015. A global analysis approach for investigating structural resilience in urban drainage systems. Water Res. 81, 15–26. https://doi.org/10.1016/j.watres.2015.05.030

Ouyang, M., Dueñas-Osorio, L., 2012. Time-dependent resilience assessment and improvement of urban infrastructure systems. Chaos 22. https://doi.org/10.1063/1.4737204

Randall, M., Fensholt, R., Zhang, Y., Jensen, M.B., 2019. Geographic object based image analysis of world view-3 imagery for urban hydrologic modelling at the catchment scale. Water (Switzerland) 11.

https://doi.org/10.3390/w11061133

Rodrigues, A.L.M., da Silva, D.D., de Menezes Filho, F.C.M., 2021. Methodology for Allocation of Best Management Practices Integrated with the Urban Landscape. Water Resour. Manag. 35, 1353–1371. https://doi.org/10.1007/s11269-021-02791-w

Song, J., Yang, R., Chang, Z., Li, W., Wu, J., 2019. Adaptation as an indicator of measuring low-impact-development effectiveness in urban flooding risk mitigation. Sci. Total Environ. 696, 133764. https://doi.org/10.1016/j.scitotenv.2019.133764

Tirpak, R.A., Winston, R.J., Simpson, I.M., Dorsey, J.D., Grimm, A.G., Pieschek, R.L., Petrovskis, E.A., Carpenter, D.D., 2021. Hydrologic impacts of retrofitted low impact development in a commercial parking lot. J. Hydrol. 592, 125773. https://doi.org/10.1016/j.jhydrol.2020.125773

Wang, S., Fu, J., Wang, H., 2019. Unified and rapid assessment of climate resilience of urban drainage system by means of resilience profile graphs for synthetic and real (persistent) rains. Water Res. 162, 11–21. https://doi.org/10.1016/j.watres.2019.06.050

Wang, Y., Meng, F., Liu, H., Zhang, C., Fu, G., 2019. Assessing catchment scale flood resilience of urban areas using a grid cell based metric. Water Res. 163, 114852. https://doi.org/10.1016/j.watres.2019.114852

Yazdanfar, Z., Sharma, A., 2015. Urban drainage system planning and design - Challenges with climate change and urbanization: A review. Water Sci. Technol. 72, 165–179. https://doi.org/10.2166/wst.2015.207

Zevenbergen, A.A., Worth, S., Dretto, D., Travers, K., 2018. Parents' experiences in a home-based dialogic reading programme. Early Child Dev. Care 188, 862–874. https://doi.org/10.1080/03004430.2016.1241775

Korea Meteorological Administration, 2020. Korean climate change assessment report 2020, Seoul, Korea. (In Korean)

Ministry of Environment (MOE), Government of the Republic of Korea. 2019. Standard guideline for design flood. Available from "www.wamis.go.kr"

Bae, C., Lee, D.K., 2020. Effects of low-impact development practices for flood events at the catchment scale in a highly developed urban area. Int. J. Disaster Risk Reduct. 44, 101412. https://doi.org/10.1016/j.ijdrr.2019.101412

De Vleeschauwer, K., Weustenraad, J., Nolf, C., Wolfs, V., De Meulder, B., Shannon, K., Willems, P., 2014. Green-blue water in the city: Quantification of impact of source control versus end-of-pipe solutions on sewer and river floods. Water Sci. Technol. 70, 1825–1837. https://doi.org/10.2166/wst.2014.306

Escuder-Bueno, I., Castillo-Rodriguez, J.T., Zechner, S., Jöbstl, C., Perales-Momparler, S., Petaccia, G., 2012. A quantitative flood risk analysis methodology for urban areas with integration of social research data. Nat. Hazards Earth Syst. Sci. 12, 2843–2863. https://doi.org/10.5194/nhess-12-2843-2012

Ghofrani, Z., Sposito, V., Faggian, R., 2017. A Comprehensive Review of Blue-Green Infrastructure Concepts. Int. J. Environ. Sustain. 6. https://doi.org/10.24102/ijes.v6i1.728

Hibbert, A.R., Troendle, C.A., 1988. Streamflow Generation by Variable Source Area 111–127. https://doi.org/10.1007/978-1-4612-3732-7_8

Horton, B.Y.R.E., 1945. MORPHOLOGY 56, 275–370.

Jajarmizadeh, M., Harun, S., Salarpour, M., 2012. A review on theoretical consideration and types of models in hydrology. J. Environ. Sci. Technol. 5, 249–261. https://doi.org/10.3923/jest.2012.249.261

Miles, B., Band, L.E., 2015. Green infrastructure stormwater management at the watershed scale: Urban variable source area and watershed capacitance. Hydrol. Process. 29, 2268–2274. https://doi.org/10.1002/hyp.10448

Petrucci, G., Rioust, E., Deroubaix, J.F., Tassin, B., 2013. Do stormwater source control policies deliver the right hydrologic outcomes? J. Hydrol. 485, 188–200. https://doi.org/10.1016/j.jhydrol.2012.06.018

Saghafian, B., Jannaty, M.H., Ezami, N., 2015. Inverse hydrograph routing optimization model based on the kinematic wave approach. Eng. Optim. 47, 1031–1042. https://doi.org/10.1080/0305215X.2014.941289

Saghafian, B., Khosroshahi, M., 2005. Unit Response Approach for Priority Determination of Flood Source Areas. J. Hydrol. Eng. 10, 270–277. https://doi.org/10.1061/(asce)1084-0699(2005)10:4(270)

Teng, J., Jakeman, A.J., Vaze, J., Croke, B.F.W., Dutta, D., Kim, S., 2017. Flood inundation modelling: A review of methods, recent advances and uncertainty analysis. Environ. Model. Softw. 90, 201–216. https://doi.org/10.1016/j.envsoft.2017.01.006

Abstract in Korean

도시 지역에서의 그린-그레이 인프라 홍수 완화 효과

배 채 영

서울대학교 대학원 협동과정 조경학,
스마트시티 글로벌 융합 전공
지도교수: 이 동 근

도시화와 기후변화로 인해 극심한 강우 빈도와 규모가 증가하고 있다. 도시 홍수는 인프라와 시민 안전에 부정적인 영향을 미치며 과도한 피해 비용을 초래할 수 있다. 따라서 도시 홍수 관리 (UFM)는 도시의 구조와 기능을 개선함으로써 홍수의 물리적 원인과 잠재적 영향을 효과적으로 관리하기 위해 필수적이다. UFM은 빗물을 관리하고 물을 처리하는 능력을 향상시키기 위해 기존 인프라와 새로운 인프라 사이의 연결과 상호작용을 고려해야 한다. 도시 홍수를 완화하기 위한 기존의 방법들은 하수도 시스템의 용적 확장에 초점을 맞추었다. 그러나 이러한 조치는 주로 지표수 처리를 목표로 하므로 예측 불가능한 강우에 대한 지속가능한 해결책이 되기 어렵다.

따라서, 자연 수문 순환을 복원하고 침투 및 유지 용량을 극대화

하여 유출을 제어하고 피크 흐름을 지연시키는 전략이 제안되고 적용되어 왔다. 이러한 전략은 국가 특성에 따라 다양한 용어 및 개념으로 제안되고 있고 용어에 따라 초점은 다소 다르지만, 생태 기술을 기반으로 하고 도시 미기후 및 생물 다양성 개선과 같은 수문학적 복원력 외에도 공공 이익을 제공한다는 데에서 목적이 같다. 본 연구에서는 기존 인프라를 강화 및 확장하는 그린인프라 (GI) 개념을 사용하였다.

본 연구에서 주로 활용되고 있는 방법론은 수문 모델인데 확률적, 경험적, 확률적, 결정론적 방법과 같은 다양한 연구 방법이 도시 홍수의 영향을 분석하기 위해 사용되고 있다. 그 중에서도 '실제'의 단순화된 표현에 기초한 수문학적 모델을 이용한 결정론적 방법은 위험 지역을 식별하거나 그린-그레이 인프라와 같은 공간 기술의 효과를 확인하는 데 적합하다. 본 연구에서는 또한 도시 지역에서 빗물이 처리되는 경계인 catchment 규모의 대상지를 구성하여 매개변수 추정 및 모델 업데이트를 기반으로 정확도를 강화한 홍수 완화 영향을 파악하고자 하였다.

이러한 방법론을 바탕으로 본 연구에서 주로 확인하고자 하는 것은 다양한 강우패턴과 공간 영향에 대한 그린-그레이 인프라의 홍수 완화 효과이다. 본 논문의 각 장에 대한 주요 연구 질문은 다음과 같다. 1) 그린인프라가 홍수 감소에 효과적인가? 2) 다양한 강우 패턴에 따

라 홍수저감 효과는 어떻게 달라지는가? 그레이 인프라와 통합했을 때 그 효과는 어떻게 달라지는가? 3) 그린-그레이 인프라 기술이 구현되는 위치에 따라 그 효과는 어떻게 달라지는가? 연구질문에 따라 제2장에서는 결정론적 모델을 기반으로 도시홍수 시뮬레이션 모델을 구축, 교정, 검증하여 결과의 정확도를 높이려 하였다. 또한 적응 전략으로서의 GI의 효과도 평가되었다. 제3장에서는 도시홍수의 회복력 개선을 논의하는 데 중요한 부분인 다양한 강우 패턴에 따른 그린-그레이 인프라 시나리오 변화에 따른 수문학적 성능 변화를 추적하였다. 제4장에서는 선행연구에서 제시한 방법론을 기반으로 도시 유역에서의 홍수 원인과 결과 영역을 탐색하여 각 영역에 그린-그레이 인프라 중 어떤 전략을 적용하는 것이 홍수 완화 측면에서 가장 효과적인지에 대한 분석을 수행하였다.

주요 연구결과는 다음과 같다. 10-30년 재현빈도의 강우강도에서 그린-그레이 인프라 모두 효과가 점차 상쇄되기 시작하였고, 50년 재현빈도 강우에서 그린-그레이 인프라 영향은 거의 제거되었다. 도시의 홍수는 일반적으로 10년 재현빈도 강우이기 때문에, GI는 많은 강우사상에서 효과적인 전략이 될 수 있다. 강우 패턴에 따라서도 홍수와 유출 사이의 감소 효과에 차이를 보였다. 지속기간이 긴 강우에서 그린-그레이 인프라의 유출 감소 효과는 낮아졌다. 다만, 홍수 감

소 효과는 반대의 결과를 보였는데 이는 고려되는 목표 지표에 따라 전략의 효과가 달라질 수 있음을 의미한다. 이는 공간적 영향 분석에서도 나타난 결과인데, 원인영역에 그린인프라를 적용하고 영향영역에 그레이 인프라를 도입하는 것이 홍수 저감 측면에서는 유리하나 유출 저감 측면에서는 두 영역에 모두 그린인프라를 설치하는 것이 유리한 것으로 나타났다.

본 연구는 도시 홍수 관리와 관련하여 기존 기반시설과 신규 기반시설 간의 상호작용을 고려할 때 바람직한 그린-그레이 인프라 계획을 위한 정보를 제공하는 데 의미가 있다. 결과는 그린-그레이 인프라 계획의 의사결정 과정에서 다양한 옵션의 상세한 비교의 중요성과 필요성을 강조한다. 특히 복잡한 도시 구조와 증가하는 강우 패턴의 변동성을 고려할 때, 본 연구의 결과는 도시홍수 관리 및 관련 정책에 유용한 시사점을 제시할 수 있을 것으로 기대한다. 다만 이 연구는 수문학적 성능에 대한 논의를 기반으로 결과를 설명하므로 의사 결정에 대한 정보를 제공하기 위해서는 비용과 관련된 함의가 필요하다.

주요어: 그린인프라, 도시 홍수 관리, 도시 배수 시스템, 결정론적 모델, 시공간적 효과

학번: 2019-35254